Journal of Experimental Psychology:
Human Perception and Performance
2001, Vol. 27, No. 5, 1163–1184

0096-1523/01/$5.00 DOI: 10.1037//0096-1523.27.5.1163

Bouncing a Ball: Tuning Into Dynamic Stability

Dagmar Sternad
The Pennsylvania State University

Marcos Duarte
Universidade de Sao Paulo

Hiromu Katsumata
The Pennsylvania State University

Stefan Schaal
University of Southern California and
Kawato Dynamic Brain Project

Rhythmically bouncing a ball with a racket was investigated and modeled with a nonlinear map. Model analyses provided a variable defining a dynamically stable solution that obviates computationally expensive corrections. Three experiments evaluated whether dynamic stability is optimized and what perceptual support is necessary for stable behavior. Two hypotheses were tested: (a) Performance is stable if racket acceleration is negative at impact, and (b) variability is lowest at an impact acceleration between -4 and -1 m/s^2. In Experiment 1 participants performed the task, eyes open or closed, bouncing a ball confined to a 1-dimensional trajectory. Experiment 2 eliminated constraints on racket and ball trajectory. Experiment 3 excluded visual or haptic information. Movements were performed with negative racket accelerations in the range of highest stability. Performance with eyes closed was more variable, leaving acceleration unaffected. With haptic information, performance was more stable than with visual information alone.

Juggling several balls in the air is a rhythmic perceptual–motor task that requires the precise timing of two hands' catching and throwing actions in continuous coordination with the balls' trajectories. The cascade pattern that beginners typically learn in their first attempt to master the art of juggling involves two hands catching and tossing three balls in the air. The hands and fingers have to grasp one or sometimes two balls and throw one of them while catching the other one with the opposite hand. However, juggling can be performed in an infinite number of variations, including bouncing the ball off the body, other objects, or the floor. In all its variety, all of these skills have one feature in common: The balls are contacted repeatedly so that they stay in the air.

One approach to understanding the coordination demands of this complex skill was advanced by Schaal, Sternad, and Atkeson (1996; Sternad, 1998, 1999). Their entry into understanding the coordinative principles of juggling (or, more generally, rhythmic ball manipulation) was to look at a single-handed bouncing of one ball with a racket. The advantage of this reduction of the skill is the elimination of complex finger and hand movements that pose challenging questions in themselves. Moreover, extended ball handling where energy is actively taken out or injected into the trajectory need not be considered. Even with this considerable simplification, the major questions of ball interception can still be addressed. To juggle or bounce a ball rhythmically in the air requires the fine control of the vertical movements of the racket in order to hit the ball with the appropriate velocity and acceleration at the right place and the right time. One additional rationale for this methodological strategy was that, in this form, the skill closely resembled a model of a bouncing ball, which has been repeatedly analyzed in the literature on nonlinear dynamics (Guckenheimer & Holmes, 1983; Tufillaro, Abbott, & Reilly, 1992). The dynamical system of a ball bouncing on a planar surface has been used as an example to demonstrate features of a nonlinear system displaying the typical characteristics of stable fixed points, bifurcations, and a period doubling route to chaos. Variations of this model still provide challenges for mathematicians and nonlinear dynamicists. The question pursued by Sternad, Schaal, and colleagues (Schaal et al., 1996; Sternad, Duarte, Katsumata, & Schaal, 2000; Sternad & Katsumata, 2000) was whether humans, when performing rhythmic ball bouncing, are guided by stability properties as identified by analyses of the nonlinear model.

In designing a task that was in deliberately close correspondence to the physical model of the one-dimensional vibratory ball–table system, Schaal et al. (1996) found support for their hypothesis that humans attune to the period-one attractor where ball and racket cycles are in a stable one-to-one relationship. This coordination strategy has the advantage that perturbations passively converge to the stable attractor, which might potentially alleviate the need for active error corrections. This strategy stands in contrast to the one advanced by the classical approach of control theory in which even the smallest deviations of a ball trajectory would have to be compensated for by an explicit change of the actuator trajectory.

Dagmar Sternad and Hiromu Katsumata, Department of Kinesiology, The Pennsylvania State University; Marcos Duarte, Escola de Educacao Fisica e Esporte, Universidade de Sao Paulo, Sao Paulo, Brazil; Stefan Schaal, Computer Science and Neuroscience, University of Southern California, and Kawato Dynamic Brain Project.

This research was supported by National Science Foundation Grant SBR 97-10312. A short poster version of these studies was presented at the International Conference for Perception and Action in Edinburgh, Scotland, August 1999.

Correspondence concerning this article should be addressed to Dagmar Sternad, Department of Kinesiology, The Pennsylvania State University, 266 Rec Hall, University Park, Pennsylvania 16802. Electronic mail may be sent to dxs48@psu.edu.

Such a control strategy has the disadvantage of demanding a high computational load on the controller, and it runs counter to the intuitive ease with which humans perform such tasks. In contrast, by exploiting the dynamically stable regime identified by the physical model of the vibratory ball–table system, there would be no need for such fine-grained error corrections. It is therefore advantageous for the performer to stay in tune with the dynamically stable solution. This is not to imply, however, that perceptual information should not be expected to also play an important role. Unlike the simulated vibratory ball–table system, the human action system is intrinsically variable. As a result, the acceleration and the orientation of the racket at impact are likely to vary from contact to contact, leading to self-inflicted deviations of the ball trajectory. Only if these deviations become too large do sensory-based corrections have to be made.

The theoretical perspective adopted here assumes that human movements are governed by attractor properties defined by the actor–environment system as a nonlinear dynamical system. The hypothesis motivating this research is that humans attune to and use stability properties of the task system and thereby find potentially more efficient movement solutions. In a broader and more historical context, this study can be viewed as an example demonstrating the propositions as laid out by Fowler and Turvey for a theory of skilled actions as early as 1978. In this programmatic article, the authors integrated propositions by Gel'fand and Tsetlin (1962, 1971), Bernstein (1967), Greene (1967, 1972), and Gibson (1966, 1979), and they provided a framework that implicitly or explicitly has influenced a wide spectrum of experimental research. The fundamental conceptual claims for a theory of acquisition and performance of skilled activity are threefold: The minimal system of analysis should be an event, encompassing both the actor and the environment as the necessary support for movements. The level of description should be course-grained and compatible with the actor's self-description and the environment. In forming a controllable system, or a coordinative structure, the actor identifies an *organizational invariant* by which the many degrees of freedom of the task are constrained. Gel'fand and Tsetlin (1962, 1971) proposed that, as such, the problem of coordination is well-organized: The variables indigenous to the specific task can be partitioned into essential and nonessential ones. Essential variables determine the topology of the solution. If an essential variable is identified, the actor can successfully search for optimal solutions in performance.

This early work has found substantial support because nonlinear dynamics has been further developed and has provided a host of formal tools to analyze the problem of coordination. Yet, although this thinking has become influential for many lines of research, few studies have explicitly captured the task with its relation between the actor's performance and environment and have identified candidates for the essential variables. We believe the research we report in this article makes such a contribution.

Overview

The previous study by Schaal et al. (1996) demonstrated, in a highly constrained experimental task, that humans do indeed attune to the dynamic stability properties of the vibratory ball–table system by optimizing the variable "acceleration at impact." In our research, we asked whether these results generalize to a less constrained ball bouncing task. To set the stage, we briefly review the modeling approach as developed and modified for studying human ball bouncing and summarize the previous results by Schaal et al. (1996). In extension of these findings, we present three experiments that test the robustness of the previous results. Central to a task-based analysis is an analysis of the perceptual contributions in establishing a certain coordinative regime. Therefore, the second major goal of this study was to examine the perceptual support that gives rise to dynamically stable behavior. Candidates for perceptual support are visual information about the ball trajectory and haptic information about the ball impact.

We present three experiments with these two goals: In Experiment 1, we relax the experimental constraints of the task by allowing participants to perform realistic racket actions to test the generality of the hypothesized strategy and the model. Furthermore, we explore the role of visual information and pursue the question of whether, in support of this stable control, anticipatory or corrective tuning through visual information can be traced. Experiment 2 goes one step further in generalizing the task and removes constraints on the ball trajectory to approximate the conditions of free ball bouncing. Experiment 3 focuses on the question of what kind of perceptual information is necessary to achieve a dynamically stable coordination strategy. We asked to what degree a dynamically stable strategy is challenged and potentially supplemented by alternative control strategies when selected perceptual information is withheld.

The Model

Bouncing a ball with a racket is modeled as a planar horizontal surface performing periodic movements in one vertical dimension impacting a ball repeatedly. This kinematic model is similar to the already classical model of the vibratory table bouncing a particle (Celaschi & Zimmermann, 1987; de Oliveira & Goncalves, 1997; Guckenheimer & Holmes, 1983; Hongler, Cartier, & Flury, 1989; Kowalik, Franaszek, & Pieranski, 1988; Pieranski & Bartolino, 1985; Pieranski, Kowalik, & Franaszek, 1985). A key difference between the studies in the mathematical literature and our approach is that in the human experiments the surface's movements have a significant amplitude and are not purely sinusoidal such that the often applied "high bounce" approximation is inadequate. This approximation in the derivation of predictions assumes that the table amplitude is negligible relative to the ball amplitude, and, therefore, assumes invariant positions of the ball–table impact with symmetric parabolic flight trajectories of the ball. Because our focus is on the table, or rather racket motions, we generalize our model equations to allow for arbitrary periodic motion of the racket. The assumptions in the formulation of the model therefore are as follows: arbitrary periodic motion of the surface, ballistic flight of the ball in a constant gravitational field, instantaneous impact modeled by a coefficient of restitution, and a mass of the racket that is considerably larger than the ball's such that the racket trajectory is not affected by the impact. The equations of motion for the ball are written in a discrete form in reference to the nth impact (see Appendix A for the derivation of the motion equations):

$$x_{B,n} = x_{R,n}$$

$$\dot{x}_{B,n+1} = -\sqrt{[(1+\alpha)\dot{x}_{R,n} - \alpha\dot{x}_{B,n}]^2 - 2g(x_{R,n+1} - x_{R,n})}$$

$$0.5gt_n^2 - [(1+\alpha)\dot{x}_{R,n} - \alpha\dot{x}_{B,n}]t_n + (x_{R,n+1} - x_{R,n}) = 0. \quad (1)$$

In this equation, $x_{B,n}$, $x_{R,n}$, $\dot{x}_{B,n}$, $\dot{x}_{R,n}$ are the vertical positions and velocities of ball and racket at the nth impact, the subscripts B and R refer to the ball and racket respectively, α is the coefficient of restitution, g is the acceleration caused by gravity, and t_n denotes the cycle time which is reset to zero at each impact (see Figure 1). During the impact, energy is lost and the system is dissipative. Therefore, according to Liouville's theorem, the system displays asymptotic stability (Lichtenberg & Lieberman, 1982). These equations are not solvable analytically because the racket's position at impact $n + 1$ is not known. However, stability analyses can be applied to find criteria under which the system achieves stable solutions. The stable solution of interest is the so-called *period-one solution,* which has one ball cycle for one racket cycle and corresponds to the task in our experiments. Other solutions of the impact map, like period-two or chaotic solutions, are not considered here.

Provided that the racket's velocity at impact $\dot{x}_{R,n}$ exceeds a minimum value to compensate for the energy loss at impact, local linear stability analysis determines at least one asymptotically stable fixed point (Strogatz, 1994; for details, see Appendix B and Schaal et al., 1996). The criterion for stability is that the racket's acceleration at impact $\ddot{x}_R$ has to satisfy the nontrivial condition

$$-2g\frac{(1+\alpha^2)}{(1+\alpha)^2} < \ddot{x}_R < 0. \quad (2)$$

Because g and α are constants, $\ddot{x}_R$ is the major variable that determines the stability of the solution. Assuming normal gravitational conditions, and setting $\alpha = .42$, which is the condition of Experiment 1, the range for stability is $\ddot{x}_R \in [-11.44, 0\ \text{m/s}^2]$. If $\alpha = .71$, which is the condition of Experiment 3 and the previously published study by Schaal et al. (1996), the range of stability is $\ddot{x}_R \in [-10.09, 0\ \text{m/s}^2]$.

This is a large range and does not yet provide very precise quantitative predictions concerning stable performance. Consequently, we performed a nonlocal Lyapunov stability analysis on Equation 1 (for details, see Appendix B). The degree of stability for 20 values of $\ddot{x}_R$ at equal intervals within the stable range is numerically determined. Figure 2 shows the results of these analyses for three values of the α parameter and $g = 9.81\ \text{m/s}^2$. The third value, $\alpha = .52$, was chosen to calculate predicted curves for

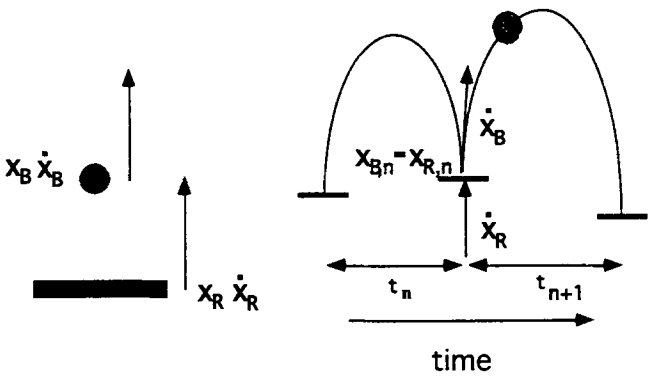

Figure 1. Sketch of the racket–ball system and the definition of variables: $x_{B,n}$, $x_{R,n}$, $\dot{x}_{B,n}$, and $\dot{x}_{R,n}$ are the vertical positions and velocities of ball and racket at the nth impact; the subscripts B and R refer to the ball and racket, respectively.

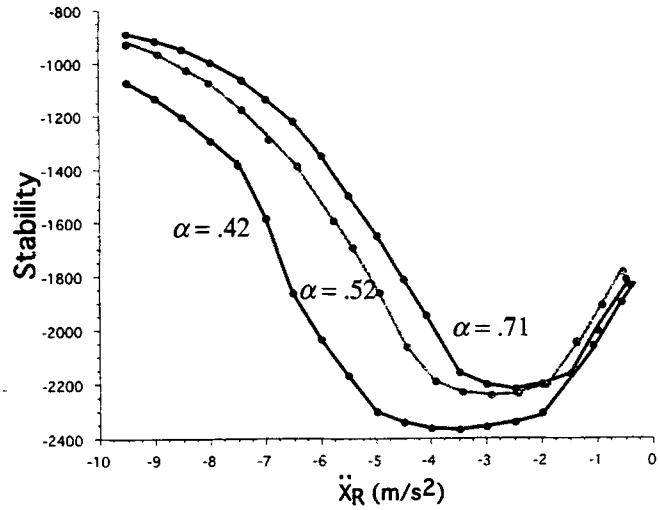

Figure 2. Results of nonlocal stability analysis, calculated for different values of α. The range of stable $\ddot{x}_R$ is determined by Equation 2. The numerical results for stability are interpreted as different levels of variability in the data. Units are arbitrary.

conditions similar to Experiment 2. As dynamic stability is closely related to variability, this numerically derived stability index serves as prediction for performance variability of the bouncing trials. Figure 2 depicts a central region where stability is highest or variability is predicted to be lowest. The smaller the coefficient of restitution, the larger the region of very high stability.

Three simulations of Equation 1 in three different regimes, presented in Figure 3, illustrate the effect of acceleration on the solutions of the model system. A perturbation is applied after the second cycle to show how the model system equilibrates or di-

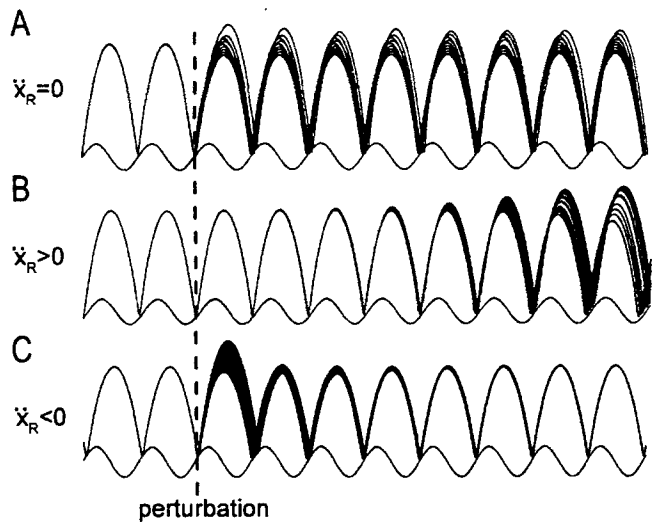

Figure 3. Simulation of Equation 1. The three runs demonstrate (A) the unstable regime, $\ddot{x}_R > 0$, where perturbations amplify; (B) the neutrally stable regime, $\ddot{x}_R = 0$, where a perturbation remains unchanged; and (C) the stable regime, $\ddot{x}_R < 0$, where perturbations converge back to the attractor.

verges: (A) When $\ddot{x}_R = 0$, the solutions are neutrally stable, and any small difference in initial conditions remains unchanged; (B) when $\ddot{x}_R > 0$, the solutions are unstable and small perturbations amplify and lead to a loss of the pattern; (C) when $\ddot{x}_R \in [-11.44, 0\ m/s^2]$, small perturbations die out and the trajectory converges back to the stable solution.

From the two stability analyses, two major conclusions can be summarized, and they serve as two predictions for the following experiments: It is hypothesized that participants perform the task with a strategy that makes use of stability properties. If they attune to stability, then the following quantitative predictions can be made:

1. Dynamically stable performance is obtained if $\ddot{x}_R$ is negative. For the specific condition of Experiment 1, where $\alpha = .42$, $\ddot{x}_R \in [-11.44, 0\ m/s^2]$. For the specific condition of Experiment 3, where $\alpha = .71$, $\ddot{x}_R \in [-10.09, 0\ m/s^2]$.

2. The degree of stability is a nonlinear function of $\ddot{x}_R$, where the highest degree of stability is found in an approximate range $\ddot{x}_R \in [-5, -2\ m/s^2]$ for Experiment 1 and $\ddot{x}_R \in [-3.5, -1.5\ m/s^2]$ for Experiment 3. By assumption, we expect the lowest variability to be found in this range.

These predictions are not trivial. Adopting the standpoint that human movements maximize efficiency, participants should contact the ball at the moment of peak velocity, corresponding to $\ddot{x}_R = 0$. Because velocity at impact is the sole determinant for ball amplitude, the moment of peak velocity in the racket trajectory leads to the highest possible amplitude given one racket trajectory. If the ball is impacted at the decelerating trajectory segment, the peak velocity has to be higher to achieve the same ball amplitude.[1]

In the previous studies Sternad and Schaal confirmed these predictions (Schaal et al., 1996; Sternad, 1998, 1999; Sternad et al., 2000). The experiment was performed with a special apparatus where participants were instructed to bounce a ball rhythmically with a steady ball amplitude by moving the handle of a 1-m-long lever arm with a racket attached at the other end. A pantograph linkage ensured that the racket's surface remained strictly horizontal. The ball was affixed to a 1-m-long boom to confine its trajectory to an approximately linear path. Hand, racket, and ball trajectories were thereby strictly confined to one vertical dimension with the explicit objective to keep close correspondence to the model. The results for six participants verified that mean $\ddot{x}_R$ across the impacts of one trial were in the range that predicted optimal stability. The variability associated with participants' mean $\ddot{x}_R$ values followed the predictions of the Lyapunov analysis.

Armed with this quantitative performance criterion, one can subsequently pose this question: What perceptual information is necessary to establish the desired task performance? The essential variable $\ddot{x}_R$ can now constitute a benchmark for exploring which kind of perceptual information establishes the link between the actor and the environment. Principal sources of information undoubtedly arise from the haptic and visual modalities. Many studies have been dedicated to assess what features of the ball trajectory are necessary for interception of the ball (Amazeen, Amazeen, Post, & Beek, 1999; van Santvoord & Beek, 1994). There is also empirical evidence that information about kinetics, specifically in collision events, can be obtained from kinematic (i.e., visual) information (Bingham, 1995; Michaels & de Vries, 1998; Runeson & Frykholm, 1983; Runeson & Vedeler, 1993; Todd & Warren, 1982). Is visual information alone sufficient to establish a stable regime? On the other hand, the haptic system has been shown to be an extremely sensitive perceptual system that uses the stress–strain patterns exerted onto muscle tissue including muscular effort in order to perceive very subtle and distant properties of the object that is contacted. Carello, Thuot, Anderson, and Turvey (1999) demonstrated that participants can detect the location of the "sweet spot" of a tennis racket by haptic information. In the experiment, blind-folded participants wielded a tennis racket and could reliably report the distance of the racket's center of percussion (sweet spot) from the hand. This and a series of similar studies highlight the ability of the haptic system of perceiving geometric (distance) and dynamic (center of percussion) properties of hand-held objects.

These previous studies motivated us to therefore ask to what degree is visual and haptic information involved in establishing a dynamically stable regime. How does the stable performance break down when participants are partially deprived of such information?

Experiment 1

Our first goal in Experiment 1 was to test whether the two central predictions of the model were satisfied when the task allowed more natural movements of the arm and the racket. In the previous experimental setup participants moved a handle of the apparatus that only allowed rotational movements around the single-degree-of-freedom elbow joint in the sagittal plane. Moreover, upward movements of the racket corresponded to downward movements of the hand moving the handle. Because of the pantograph linkage, any tilting of the racket was excluded. Could it be that this apparatus imposed such tight and specific constraints that participants had no choice but to bounce the ball at negative accelerations? To test whether the predicted stable strategy was maintained in a less constrained juggling task, we removed the pantograph apparatus and participants performed the bouncing movements holding a tennis racket in their hands, with no explicit constraints on the arm or racket movements. However, the ball still remained attached to a boom and was thereby confined to an approximately linear path, so the task remained essentially limited to one vertical dimension and retained sufficient correspondence to the model.

Our second goal in this study was to investigate the role of visual information for a dynamically stable performance of ball bouncing. With the objective of a task-based analysis, where coordination is assumed to arise from the relation between actor and environment, our immediate question was the following: What

[1] The biomechanical literature on ball hitting or kicking typically studies single contacts that aim to maximize ball amplitude or precision, such as in baseball or tennis. Therefore, these analyses aim to identify how speed is maximized at the distal end of the kinematic chain of the limb. The effectiveness of the summation of segmental velocities is evaluated by the manner with which each body segment moves with respect to the more proximal segment (Elliott, 2000; Herring & Chapman, 1982; Hubbard, Covarrubias, Hagenau, & Jenssen, 1989). The central requirement of a periodic impact in our ball bouncing task imposes different criteria for the optimal type of impact. It is therefore important to point out that the predictions from the performed stability analyses only make predictions about rhythmic bouncing, hitting, or kicking. Transfer of the present predictions to single impacts as in tennis, where the nonidentical nature of each successive impact is of primary importance, is not valid.

kind of perceptual information establishes the link between actor and environment? Our first step in this direction was modest: We tested whether visual information about the ball and racket movements was needed to ensure the same dynamically stable behavior. Given that when a stable strategy is established performance can theoretically be successful without corrective adjustments, the expectation was that performance should be equally possible when visual information was partially withheld. If this was not the case, then this result speaks to the presence of additional corrective adjustments.

Method

Participants

Six participants (3 women and 3 men) from the undergraduate and graduate student population of The Pennsylvania State University volunteered. Their average age was 31.7 years, and none of them reported any arm injuries. All of the students had some experience with racket sports. They signed an informed consent form in accordance with the Regulatory Compliance Office of the university.

Apparatus and Materials

The bouncing movement was performed with a custom-made apparatus that consisted of three measurement parts: one potentiometer measuring the vertical displacement of the racket, a second potentiometer that measured the displacement of the ball, and an accelerometer that was attached to the racket (Figure 4). To measure the vertical displacement of the racket, a thin string was tied to the center of the racket surface. The other end of the string was attached to a floor piece, which consisted of a wheel that rotated around a horizontal axle, which was in turn fixed to a heavy steel floor board (.41 m × .18 m × .02 m) weighing 30 kg. The string from the racket was fixed to the wheel and was wound around because of a horizontally located spring that turned the wheel to a resting position. Vertical movements unreeled the string against a small resistance from the spring and turned the wheel. A 10-turn potentiometer at the axle measured the turns of the wheel and thereby the vertical displacement of the racket. A sufficient degree of tension on the string was obtained through a spring that could be adjusted manually by turning it so that the racket movements neither confronted too much resistance nor created any slack in the string. As the position of the racket was directed at the ball (which was at a constant position in the horizontal plane), the racket's movements were always close to vertical in successful bouncing. Before data collection the experimenter ensured that the wheel was positioned directly underneath the sweet spot of the racket.

The ball was fixed to a 1.12-m-long tube made of carbon fiber with a diameter of 20 mm and wall thickness of 0.5 mm. This material was chosen to ensure minimal weight of the boom combined with maximal stiffness so that the tube and the attached ball would not vibrate after impacts. The tube was connected to a pivot on the vertical stanchion. At the short end of the boom (.15 m), a weight of 0.20 kg was attached to offset the weight of the tube. This corresponded to a change of gravity for the ball's ballistic flight. Change of this weight allowed for the experimental manipulation of gravity in the previous experiment. Because of the rigid linkage of the ball to the boom, the trajectory of the ball described a curvilinear path. In first approximation the ball's trajectory traversed a $\pm 30°$ angle such that the ball's trajectories were treated as linear. The second potentiometer was attached to the hinge joint between boom and stanchion and measured the rotational movements of the boom. To obtain data for the ball's movements, we converted these rotational displacements into vertical movements of the ball. At the base of the racket's handle a uniaxial accelerometer (Coulbourn Instruments, Allentown, PA) was affixed. All analog data were digitized using a 16-bit A/D board (National Instruments, Austin, Texas) and sampled at 500 Hz using software developed in LabView (National Instruments, Austin, Texas). The three separate signals were time aligned by the software. The ball was a squash ball, and the racket was a regular tennis racket with an average-sized frame and normal string tension. The coefficient of restitution α of this ball and racket system was

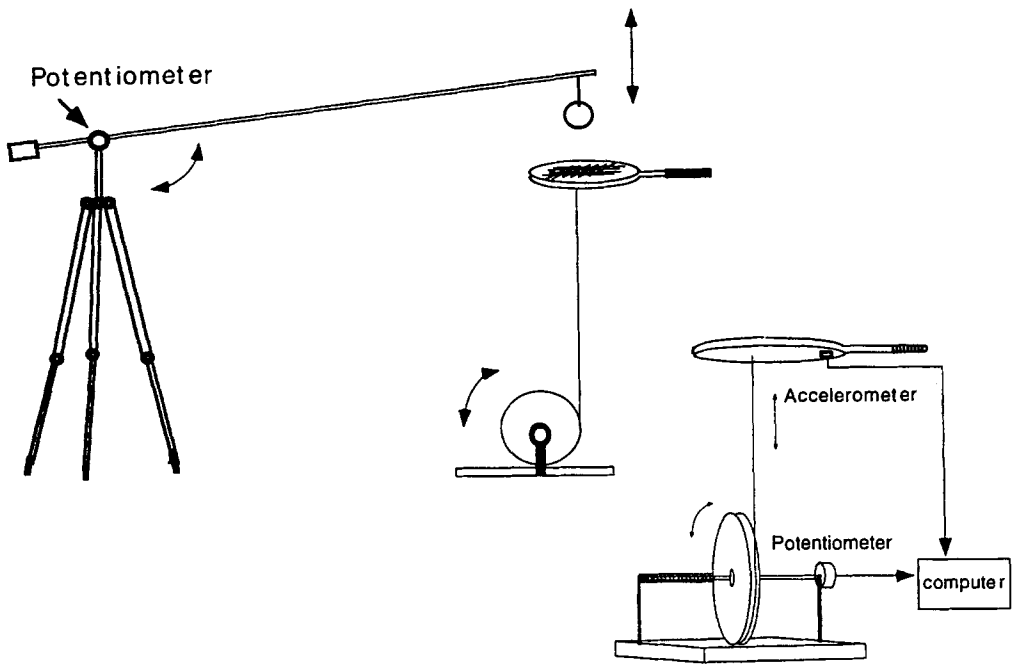

Figure 4. Experimental apparatus of Experiment 1. See the text for details.

determined empirically by recording a range of ball velocities before and after the impact. For the first experiment, $\alpha = .42$.

Procedure and Design

At the beginning of each experimental session, the participants were asked to practice the task for approximately 5 min, which proved sufficient to get acclimated to the apparatus, the weight of the racket, and the range of amplitudes that were possible with the apparatus. Participants were instructed to bounce the ball at a constant ball amplitude within each trial. In a given trial, participants were instructed to bounce the ball at either low, medium, or high ball amplitude rhythmically throughout one trial. During the practice, participants were asked to select their own set of three distinguishable amplitudes. No target amplitudes were given visually. *Medium amplitude* was defined to be the height at which each participant preferred to juggle the ball. *Low amplitude juggling* was described to the participants to be "as low as possible, without letting the ball merely vibrate on the racket" and, thus, it still required active control over the ball. *High amplitude* was defined as a high but still comfortable range. When bouncing the ball high, participants were made aware that they should not get into the curvilinear range of the ball's trajectory, which was at an approximate elevation of 0.50 m measured from the horizontal position of the boom.

The experimental session consisted of two blocks. In the first block participants performed the task with their eyes open, whereas in the second they performed with their eyes closed. Three trials at each amplitude condition were presented in random order. In the second block participants were asked to close their eyes only after having established a stable movement pattern. The two blocks with the two perceptual conditions were always presented in the same order because the eyes-closed condition was expected to be more difficult. All trials were performed with the racket held in the dominant hand. Each of the 18 trials lasted 30 s, and the total experiment lasted approximately 25 min. Participants could rest their arm between trials whenever they wanted. Each trial began with the participant starting the movement, and when the participant felt that a stable pattern was established, he or she signaled to the experimenter and the data collection was started. If a participant lost the pattern (e.g., the ball remained on the racket), the trial was repeated. This happened only twice.

Data Collection and Reduction

The position data of the racket were low-pass filtered using a zero-lag second-order Butterworth filter with a cutoff frequency of 12 Hz. This cutoff frequency was chosen to eliminate measurement noise while preserving modulations in the participant's performance. The signal was differentiated with a simple difference algorithm and subsequently filtered again using the same filter parameters. Of central interest was the value of acceleration at the moment of the racket's impact with the ball. The signal from the accelerometer was not filtered because the discontinuous point of impact was of focal interest. The determination of this point was straightforward because the acceleration had a sharp discontinuity at the moment of impact. The value before this discontinuity was picked as an estimate of the acceleration of the racket just before impact.

To capture more systematic features within each cycle of the racket and ball trajectory, we defined two further measures on the basis of the continuous trajectories.

Harmonicity. We defined a so-called harmonicity measure λ to capture the racket trajectory's deviation from a harmonic wave. To this end, we analyzed the racket trajectory in phase space, defined by both its state variables position and velocity. First, phase θ_R and radius r were calculated from the limit cycle of the racket trajectory following standard methods (for more detail, see Sternad, Turvey, & Saltzman, 1999):

$$\theta_R = -\arctan\left[\frac{(\dot{x}_R - \bar{\dot{x}}_R)T_R/2\pi}{x_R - \bar{x}_R}\right] + \pi,$$

where $\bar{x}_R$, $\bar{\dot{x}}_R$, and $\bar{T}_R$ refer to the average position, velocity, and period of one trial's trajectory, respectively. Phase θ_R was defined to be zero at the maximum position of the racket trajectory. The phase for the ball trajectory θ_B was defined in analogous fashion as zero at the maximum of the ball's trajectory. The radius $r(t)$ in phase space of the racket trajectory was computed as

$$r(t) = \sqrt{x_R^2 + (\dot{x}_R T_R/2\pi)^2}.$$

As a harmonic wave traverses a unit cycle in phase space, we captured the degree of harmonicity of the racket trajectory's periodic motion as its deviation from a unit circle. Then, we normalized r to 1 and determined λ as the difference between r and 1. To obtain a characteristic profile of λ per cycle, we divided the r signal into cycles of 2π length as captured by their phase and plotted r as a function of the cycle's phase. We divided each cycle into 36 bins of $2\pi/36$ radians length. For each bin, the λ values of all cycle segments were averaged and their variances (V) determined. To facilitate a quantitative comparison across conditions, we defined the cumulative measure λ_{MSE} as follows:

$$\lambda_{MSE} = \sqrt{\frac{\sum_{n}^{36} V_n \lambda}{36}}.$$

Relative phase. We determined the relative phase between ball and racket movement. The basis for this measure were the time series of both θ_B and θ_R. Relative phase ϕ was defined as $\phi = \theta_B - \theta_R \bmod 2\pi$.

As above, the continuous time series of ϕ was segmented into cycles on the basis of θ_R, divided into 36 bins and averages and standard deviations determined for each bin. The average ϕ per cycle captured the mean relative behavior throughout a cycle. Furthermore, and similar to λ_{MSE}, we quantified fluctuations around mean ϕ in terms of a root mean square measure ϕ_{MSE}:

$$\phi_{MSE} = \sqrt{\frac{\sum_{n}^{36} V_n \phi}{36}}.$$

Results and Discussion

Task Criterion: Ball Amplitude

Our first aim was to ascertain whether participants followed the instructions and actually performed the ball bouncing task with three different and relatively invariant ball trajectories. Trial averages of the relative ball amplitudes A_B and their standard deviations $SD(A_B)$ were submitted to a $3 \times 2 \times 3$ repeated measures analysis of variance (ANOVA) with the factors amplitude, perceptual information, and repetition. Results confirmed that participants performed the task at three distinguishable amplitudes, $F(2, 10) = 128.48$, $p < .0001$, where the mean peak heights were .36 ± .04 m, .18 ± .03 m, and .10 ± .02 m. A significant main effect for perceptual information indicated that in the eyes-closed condition, the amplitudes were lower than in the eyes-open condition, $F(1, 5) = 31.56$, $p < .01$ (see Table 1). An interaction between visual information and amplitude indicated that the differences between the perceptual conditions were less marked for low amplitudes compared to high amplitudes, $F(2, 10) = 17.24$, $p < .001$.

The standard deviations around A_B, $SD(A_B)$ were submitted to the same ANOVA. Variability was highest for the high amplitude conditions and decreased successively for the medium and low

Table 1
Means (and Standard Deviations) for Racket and Ball Periods T_R and T_B (in Seconds) and Amplitudes A_R and A_B (in Meters) in Experiment 1

Condition	T_R	T_B	A_R	A_B
Open eyes				
High	0.82 (0.04)	0.82 (0.04)	0.32 (0.03)	0.36 (0.04)
Medium	0.60 (0.03)	0.60 (0.03)	0.18 (0.02)	0.18 (0.03)
Low	0.46 (0.04)	0.46 (0.05)	0.10 (0.01)	0.10 (0.02)
Closed eyes				
High	0.74 (0.04)	0.74 (0.04)	0.26 (0.02)	0.27 (0.04)
Medium	0.56 (0.03)	0.56 (0.04)	0.16 (0.02)	0.15 (0.03)
Low	0.46 (0.04)	0.47 (0.06)	0.10 (0.01)	0.10 (0.02)

amplitude conditions, $F(2, 10) = 20.36$, $p < .001$. There was no effect for perceptual information, which indicated that the accuracy in following the task instructions was similarly good with and without visual information. Most likely, this was due to the highly predictable ball path. Haptic and auditory information may play an important complementary role in achieving a regular ball amplitude.

Model Predictions: Racket Acceleration at Impact

The variable that directly addressed the central question of this study was the acceleration of the racket at impact $\ddot{x}_R$. As derived from the model above, $\ddot{x}_R$ served as the criterion whether participants performed the bouncing movements with a parameterization that provided dynamic stability. Figure 5A shows the trial means of the six participants in all experimental conditions: All $\ddot{x}_R$ values scattered across a range of -6.80 and $+1.55$ m/s^2, with the overall mean at -3.16 m/s^2. Six trials had $\ddot{x}_R$ in the positive range. The superimposed line represented the model predictions from the nonlocal stability analysis, showing that the approximate range of $\ddot{x}_R$ values with lowest predicted stability was approximately between -5 and -2 m/s^2. The scattergram and the inserted histogram of $\ddot{x}_R$ values with its median at -3.40 m/s^2 confirmed that the data were in good qualitative and quantitative agreement with the predictions. Note that, again, positive values were possible and that the predominance of negative $\ddot{x}_R$ was not a trivial finding. In summary, this result confirmed the first prediction that participants again bounced the ball with negative $\ddot{x}_R$, even when the task was less constrained.

The next analysis assessed whether the mean $\ddot{x}_R$ values differed between the experimental conditions, with a special focus on the effect of the presence or absence of visual information. To this end, all trial averages were submitted to a 3 × 2 × 3 ANOVA with the factors amplitude, perceptual information, and repetition. An interaction between amplitude and perceptual information was significant, $F(2, 4) = 4.06$, $p = .051$. This trend indicated that for the eyes-closed condition all values were relatively similar, whereas in the eyes-open condition the acceleration was significantly more negative than in the high amplitude compared to the low amplitude condition. The overall mean racket acceleration differed significantly between the amplitudes, $F(2, 10) = 8.37$, $p < .01$ (high: $\ddot{x}_R = -4.04$ m/s^2; medium: -3.24 m/s^2; low: -2.22 m/s^2). A second main effect was obtained for repetition, $F(2, 10) = 7.96$, $p < .01$, where the overall means decreased progressively: First trial: $\ddot{x}_R = -2.84$ m/s^2; second trial: -3.24 m/s^2; third trial: -3.43 m/s^2. The comparison between the two conditions with visual information present or withheld was not significant ($p = .86$). The first main effect is at first sight counterintuitive. In order to achieve higher ball amplitudes, higher velocities at impact are required. However, participants appeared to have lost more

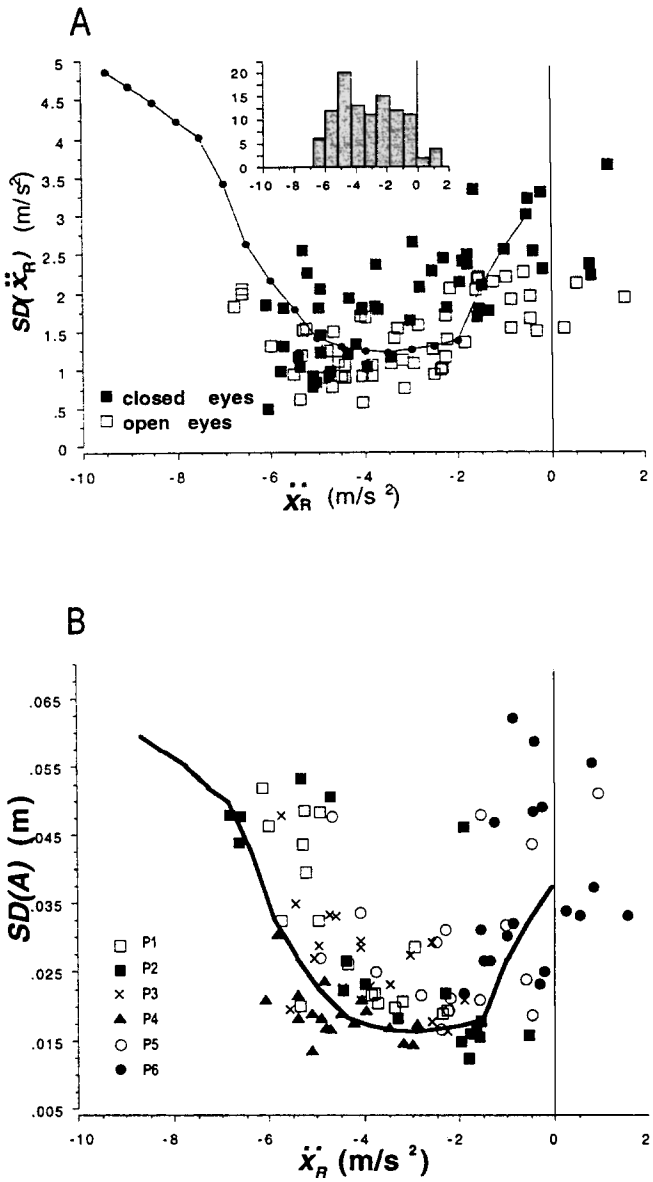

Figure 5. $SD(\ddot{x}_R)$ versus trial means of $\ddot{x}_R$ of Experiment 1. A: Trial means of all participants' acceleration of the racket at the moment of impact are plotted against the standard deviations around each trial mean. The different symbols represent the two perceptual conditions. The inserted histogram shows the frequency of x_R for different values of x_R. The solid line represents the predicted degree of stability as calculated from the nonlocal Lyapunov stability analysis. (The simulations results were in arbitrary units; therefore, the units were scaled to fit the experimental data.) B: Variability estimates $SD(A_B)$ against $\ddot{x}_R$. The different symbols represent the 6 participants, showing that each participant had a preferred range in the defined space.

velocity; they were already decelerating when they impacted the ball. From an efficiency standpoint, participants would be expected to perform high amplitude bouncing with impacts closer to peak velocity in their racket cycle. Instead, participants chose to increase the racket amplitude and then had to slow down the upward movement from higher peak velocities, thereby requiring higher decelerations. To confirm and further examine these within-cycle features, we discuss more fine-grained analyses of the racket trajectory below.

The second main effect concerning the effect of visual information was important with respect to the second objective of the experiment. Indeed, participants continued to bounce the ball with the same strategy, choosing impacts at moments in the trajectory where acceleration was negative. This suggests that visual information did not play a significant role in detecting and maintaining the stable regime. Recall, however, that in the present task, the ball was affixed to a long boom and its trajectory was highly predictable. The only positional adjustment necessary for the racket was in the vertical position—which, however, determined the value of the acceleration at impact. More insights into these results are provided by analyses of the continuous ball and racket trajectories.

The third main effect for repetition indicated that with increasing practice of the task, participants chose increasingly more negative racket accelerations (Figure 6). This result indirectly speaks to the fact that with practice, participants gravitated toward values that provided more stability.

Stability and Variability of Racket Acceleration

The next important question focused on the prediction that dynamically stable solutions are accompanied by lower variability. The degree of stability was operationalized by calculating the standard deviations of the successive values of $\ddot{x}_R$ throughout one trial, $SD\ddot{x}_R$. The estimates of $\ddot{x}_R$ and $SD\ddot{x}_R$ per trial were plotted against each other in Figure 5A. The solid line represents the relative stability associated with different values of $\ddot{x}_R$. Note that the values on the ordinate of the prediction are in arbitrary units from the numerical analysis (cf. Figure 2). Therefore, the predicted curve was scaled into the data and does not allow a quantitative comparison in the ordinate dimension. With this caveat in mind, the data give a good qualitative fit of the predictions derived from the model. To establish that the curve was more appropriate than

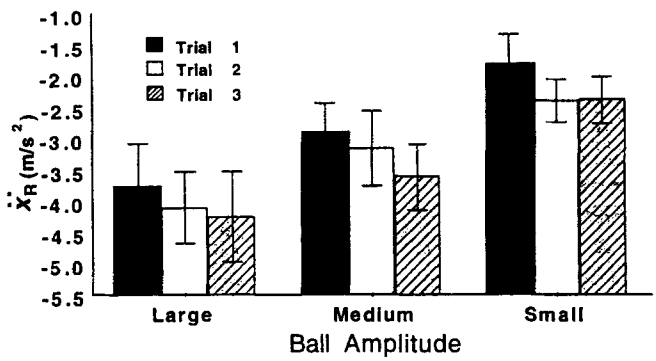

Figure 6. Mean racket accelerations at impact for the three ball amplitudes and the three trials per condition. The error bars denote standard errors.

a simple linear dependency, we also performed a second-order polynomial regression. The r^2 value of the fit was .31 and significant ($p < .0001$). The second-order coefficient was significant at the 5% level, indicating that the scatter of data was better accounted for by a curved fit rather than a linear fit. To further emphasize that the variability in the performance in different trials followed the stability predictions, we also plotted the $SD(A_B)$ against $\ddot{x}_R$. Figure 5B clearly shows that the scatter of data followed the predicted U shape. The different symbols in the figure denote the different participants (P1, P2, . . .).

The trial estimates of $SD\ddot{x}_R$ were submitted to the same repeated-measures ANOVA as above. A two-way interaction between amplitude and repetition was significant, $F(4, 10) = 3.19$, $p < .05$, showing that $SD\ddot{x}_R$ decreased in trials with high to medium amplitude but remained at the same level for the low amplitude conditions. A main effect for visual information supported the intuitive expectation that the eyes-closed condition was more variable than the eyes-open condition, dropping from .20 m/s^2 to .15 m/s^2, $F(1, 5) = 15.01$, $p < .05$ (see Figure 5A). Inspecting the individual condition averages also explained why variability did not show the expected decrease over the three repetitions. In the low amplitude condition, the variability did not change across the repetitions. In summary, with respect to the second question about the role of visual information, the actual value of the critical variable did not change, but variability was affected by the absence of visual information. This suggests that visual information about the ball and racket was involved in stabilizing the ball trajectory. To further examine how visual information leads to changes in the racket trajectory, we next turn to the analysis of the continuous time series.

Analysis of Continuous Trajectories: Harmonicity

All preceding analyses focussed on the analysis of the impact alone; they directly tested the predictions, which were derived from the analysis of the discrete model. Given the emphasis that coordination implies a perceptual link between environmental support and the actor, we next ask how this stable regime is brought about. Are there discernible signs in the continuous racket trajectory speaking to active corrective control? To scrutinize in what way the racket trajectories differed throughout the cycle, we examined them in terms of their harmonicity, that is, the degree to which they differed from a harmonic wave. The overarching goal was again to detect differences in strategy across the different manipulations as well as in trials deemed stable or unstable according to the critical variable $\ddot{x}_R$.

Figure 7 shows the harmonicity measure λ for six representative trials in the six experimental conditions performed by 1 participant. As detailed in the Method section, λ is graphed as a function of the phase of the racket cycle θ_R. Because of this plotting, the successive cycles were normalized to 2π and pooled in 36 bins to obtain an average profile. The error bars show standard deviations for each of the 36 bins. Phase zero is at the maximum of the racket trajectory. As evident from all six panels in Figure 7, λ showed a characteristic shape that was only modified in scale across the amplitude variations. For large amplitudes the deviations from harmonicity were most marked. For λ, values larger than zero imply that position and velocity, alone or in conjunction, were increased. Conversely, λ values smaller than zero, as observed in

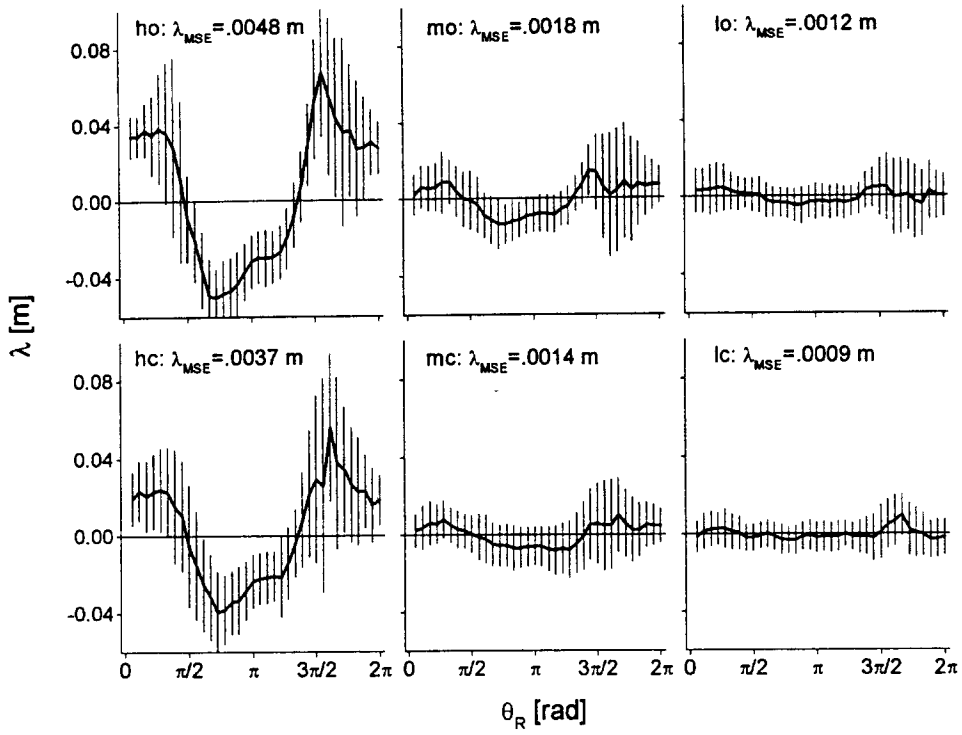

Figure 7. Harmonicity measure λ in six combinations of conditions. The top three trials are trials performed with eyes open (o). The bottom three graphs are trials performed with eyes closed (c). From left to right: high (h), medium (m), and low (l) amplitude. The λ_{MSE} for each trial is listed on the top of each graph. The error bars denote the standard deviations for each of the 36 bins.

the central part of the cycle, signify that position and velocity were decreased. The peak of λ at about $3/2\pi$ was coincident with the moment of impact, indicating a marked deviation from a harmonic cycle. The interval with negative λ leading up to the peak was possibly due to anticipatory adjustments before the impact. This regular pattern is the signature of an asymmetric periodic trajectory consisting of a slower and a faster portion. Interestingly, no striking differences in shape were seen between the two perceptual conditions, suggesting that visual information did not play a dominant role in the task performance.

The summary measure λ_{MSE} was defined as the cumulative difference between the trajectory and a harmonic wave in the different experimental conditions. Using an ANOVA performed on λ_{MSE} we obtained the following results: An interaction between amplitude and visual information indicated that for high amplitudes performed with eyes open, λ_{MSE} was significantly higher than in all other conditions, $F(2, 10) = 19.09$, $p < .0001$. There was a main effect of amplitude, corroborating the effect seen in Figure 7 that in the high ball amplitude conditions λ deviated more strongly from a sinusoidal wave than in the medium and the low amplitude conditions, $F(2, 10) = 36.92$, $p < .0001$. There was also an effect of perceptual information, indicating that with their eyes open participants tended to deviate more from a sinusoidal wave than without visual information, $F(1, 5) = 60.16$, $p < .001$. In summary, the racket trajectories deviated more from harmonicity in high bouncing amplitudes compared to low amplitudes. When participants had their eyes closed, they tended to move the racket in a more harmonic fashion than when they had visual information about the ball's trajectory. This result is consistent with the earlier result that on average, racket amplitudes were smaller when participants had no visual information. That is, the difference in λ_{MSE} between perceptual conditions may have been merely a by-product of different magnitudes of racket amplitudes.

Relative Phase

Figure 8 shows the average relative phase ϕ per cycle and its band of standard deviations plotted against θ_R for the six different experimental conditions performed by the same participant. Inspection of the time course of ϕ immediately shows again that there was a typical profile throughout one cycle, which was invariant for all six conditions. The profile varied around a mean of $-\pi/2$, which corresponds to the racket leading the ball by a quarter of a cycle. The discontinuous change in ϕ around $3/2\pi$ is the moment of impact. Note that both θ_R and θ_B were defined to be zero at peak amplitude, which leads to this constant phase difference. Moreover, the two trajectories of ball and racket are different, so ϕ is never a constant value. To better interpret the expected shape of ϕ, the model system, which consisted of a sinusoidal racket trajectory and a parabolic flight of the ball, was simulated and trajectories were generated. The insert in the top left graph shows the simulated ϕ calculated from this model in the same way as for the data. Assuming no change from sinusoidal motion, ϕ decreases in a nonlinear fashion up to the impact event. It changes discontinuously at a racket phase close to $3\pi/2$. Although ϕ of the

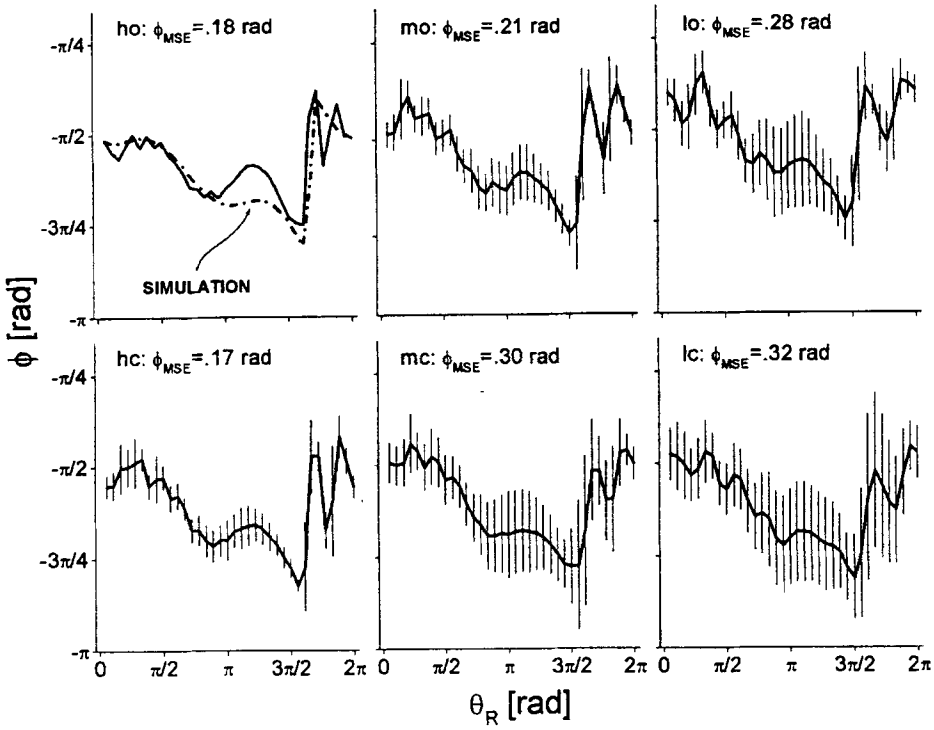

Figure 8. Relative phase ϕ determined for the six combinations of conditions. The top three panels present trials performed with eyes open (o). The bottom three panels present trials performed with eyes closed (c). From left to right: high (h), medium (m), and low (l) amplitude. The error bars denote the standard deviations for each of the 36 bins.

data closely follows the simulated trajectory for the first half of the cycle, it deviates markedly for a quarter cycle prior to the impact. This phase of the trajectory concurs with higher standard deviations as can be read from the other five panels. This illustrates that there is a crucial phase where the ball impact is prepared and variability during this phase is higher.

To quantify whether there were differences in the relative phase across conditions, we defined the quantity ϕ_{MSE}. Conducting an analysis of variance on ϕ_{MSE}, we detected only one weak but significant difference between the three amplitude conditions, $F(2, 10) = 4.75$, $p < .05$. It showed that the low amplitude had a significantly higher ϕ_{MSE} than the medium and high amplitudes.

To conclude, Experiment 1 provided a number of results: The first objective of the present line of experiments was whether the simple mechanical model provided a robust framework to understand the task of rhythmically bouncing a ball. The unambiguous answer to this question is yes. In the majority of trials, the ball–racket impact occurred in the decelerating part of the racket trajectory, that is, in the dynamically stable regime as predicted by the model. Moreover, across three repetitions, the acceleration values changed toward ones that, according to the model, provided greater stability. To further corroborate the relevance of these predictions, the variability associated with different parameterizations concurred with the differential stability predictions.

The second focus of inquiry was directed to explore the role of perceptual information in achieving this perceptual–motor task, and especially how to perform it with a dynamically stable strategy. The results gave a mixed picture: The comparison between the eyes-open and eyes-closed conditions did not produce a difference in the racket acceleration. This suggests that dynamic stability can be obtained by other kinds of perceptual information, such as haptic information. On the other hand, there were differences in the variability measures in that the eyes-closed condition was more variable. This result suggests that visual information, when present, was used in either anticipatory or corrective fashion. It appears that small deviations can be absorbed in the dynamically stable regime but that larger deviations are compensated for on the basis of visual information. Analyses of the continuous racket movement profiles further suggested signs of anticipatory adaptations. Both measures of harmonicity and relative phase between ball and racket indicated that approximately a quarter cycle before impact the trajectory clearly deviated from a harmonic wave, indicating preparatory action for the ball contact. In the blindfolded case, these anticipatory actions may rely on cycle timing. Furthermore, variability around the mean relative phase and harmonicity was increased, speaking to a fine-tuning prior to impact (Bootsma & van Wieringen, 1990). However, no differences could be found between the two visual conditions or between trials performed with positive or negative acceleration. Given these results, Experiment 1 was the departure point for two more experiments in which we pursue the issues of the generalization of the task and the role of perceptual information.

Experiment 2

One major result of Experiment 1 was that although the ball bouncing task was less constrained than the model, participants

again chose movement solutions consistent with the criteria for a dynamically stable solution. The theoretical predictions of the proposed model and the results obtained from the initial experiment proved to be robust even when the impacting surface was not strictly horizontal and the movement was performed with the whole arm. Experiment 2 pursued this issue one step further and removed more constraints on the task. The participants now performed ball bouncing freely in 3D.

Method

Participants

Five right-handed individuals (3 men and 2 women) volunteered for this experiment. Four of them were graduate students and 1 (a woman) was an undergraduate student of The Pennsylvania State University. Their ages ranged from 21 to 36 years (M = 29.8 years). Four of them had already participated in the earlier experiment and were familiar with racket sports. The only exception was the undergraduate student who had no prior experience with racket sports outside the experiment. Before data collection, the participants gave their informed consent in accordance with the University Regulatory Compliance Office.

Apparatus and Materials

The experiment used the same tennis racket with the attached accelerometer as in Experiment 1. The central modification was that the ball was no longer attached to the boom but was bounced freely in 3-D. To facilitate this spatially unconstrained bouncing, the racket was also no longer attached to the floor piece with the string. The accelerometer had a long cable connecting it to the computer, so that the racket movements were not obstructed and were truly performed in 3-D. However, no position data of ball and racket were collected. A sponge ball the size of a tennis ball was used, which was lighter and easier to control. The exact coefficient of restitution could not be determined because there was no position data available to measure ball displacements and velocities before and after the impact. However, when the ball was attached to the boom α was determined to be .52. Gravity conditions were therefore normal, g = 9.81 m/s^2. The acceleration data were collected by the same A/D card and LabView software as in Experiment 1. The sampling rate was 500 Hz.

Procedure and Design

Before we started the data collection the participants had the opportunity to practice for as long as they wanted to get used to the apparatus and task. The racket was slightly heavier because of the attached accelerometer, but otherwise the task did not differ from the normal movement with a tennis racket. Ten minutes of practice usually sufficed in which participants tried out different bouncing amplitudes. They were told to find their most comfortable ball amplitude. They were also instructed to stay as stationary as possible and not to move more than one step to reach the ball when it was displaced slightly. No standing area was prescribed. Because our focus was on testing the validity of the model predictions for the unconstrained task, we refrained from collecting different amplitude conditions, and so a finer grained analysis of the position data was not possible. Furthermore, the ball's trajectory was now completely unconstrained, so the task had to be performed with open eyes. Performance with closed eyes was possible but very difficult.

Participants began to bounce the ball by themselves. When they had settled into a stable pattern at their preferred frequency, they signaled to the experimenter to start the data collection. If they had to step for more than one step or lost the ball, the trial was repeated. For some participants, especially the female undergraduate who had no experience with racket sports, this happened a couple of times. Most other students had no problems in maintaining a stable pattern. Participants performed four trials in succession with a few minutes break in between, following the same instruction. Each trial lasted 30 s.

Data Analysis and Reduction

The racket acceleration at impact was determined on the basis of the unfiltered signals as in Experiment 1. In addition, the intervals between impacts in the acceleration signal provided a measure of the periodicity of the rhythmic performance. Prior to capturing the central tendency and dispersion of these two measures per trial, we checked the distribution of the 40 to 60 data points and found that many trials did not satisfy a normal distribution. We therefore calculated the median and interquartile range of the dependent measures to describe individual trial performances across one trial.

Results and Discussion

The self-selected periods for this task ranged between individual trial medians of .308 s and .647 s, with an overall arithmetic mean of .502 s. The range of period values per trial were on average .027 s, indicating that participants fulfilled the task demands and bounced the ball at a relatively steady rhythm and, consequently, with a relatively stable ball amplitude. This is an informative result as the task was relatively demanding compared with the one in Experiment 1; in the present task the ball could actually be lost. The variability estimates did not show any systematic dependencies on the median periods. Each participant produced very similar periods in the four trials.

The primary focus in this experiment was again on the racket accelerations at impact $\ddot{x}_R$. Participants performed trials with median $\ddot{x}_R$ values ranging between -4.10 and -0.54 m/s^2. As summarized in Figure 9, different participants (P1, P2, . . .) had trial means around different $\ddot{x}_R$ values that reflected different preferences, which repeated the picture obtained from Experiment 1 (compare Figure 5). This result confirmed that model's predictions were again satisfied. What is noticeable, however, is that $\ddot{x}_R$ values were confined to a smaller range than previously. As was seen in Figure 2, the smaller the alpha, the shorter the range, or the smaller the "well" providing optimal stability.

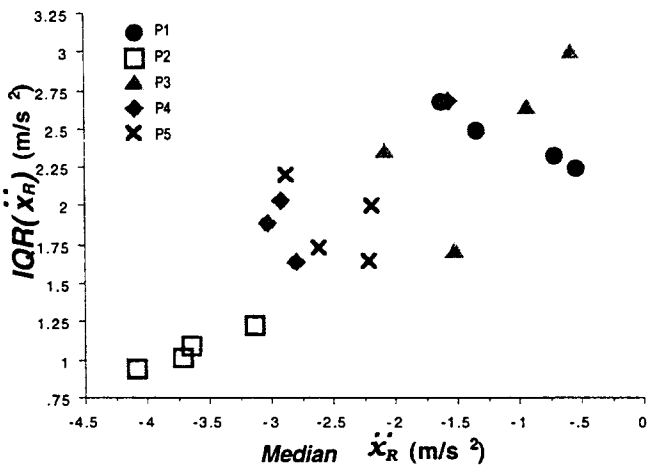

Figure 9. Interquartile range (IQR) of $\ddot{x}_R$ versus trial medians of $\ddot{x}_R$ of Experiment 2. The different symbols represent the 5 participants.

To test the predictions for stability associated with different $\dot{x}_R$ values, the same qualitative picture as in Experiment 1 emerged. Variability quantified by the interquartile range of $\dot{x}_R$ consistently decreased with increasingly negative $\dot{x}_R$ values (Figure 9).

The major conclusion from this study is that even in completely unconstrained performance the task was again performed with a strategy such that the racket's upward movement was already in its decelerating phase when hitting the ball. As argued above, the selection of this specific strategy is not trivial and runs counter to an alternative strategy where the ball is hit at peak velocity that could be deemed a more efficient strategy. We therefore conclude that the model has validity even when the movement task is far less constrained than its original one-dimensional formulation. Consequently, the results support our claim that participants attuned to a strategy that used the stability properties of the task.

Experiment 3

The second major objective of our experimental series was to determine what kind of perceptual information is necessary for actors to attune to the identified stable movement strategy. Experiment 1 showed that for the one-dimensional task, visual information was not critical and, on the whole, performance (as captured by the essential variable $\dot{x}_R$) was indistinguishable regardless of whether visual information was available. On the other hand, variability in $\dot{x}_R$ did differ for the two visual conditions. This result can be interpreted in two ways: Either visual information is not needed for attaining dynamically stable performance, or other informational sources provide the relevant information that couple the actor and the environment. If perceptual information were not needed for maintaining stable performance, this would support the hypothesis that rhythmic ball bouncing can be maintained without ongoing adjustments. Alternatively, there may be other information that aids in maintaining the performance. Given the centrality of the impact in this task, our conjecture was that haptic information is at least as important as visual information. This includes information about the force at the impact as well as kinesthetic information about the continuous arm movements leading toward the impact. We designed Experiment 3 to shed more light on the relative contribution of the sensory modalities to performance. An apparatus was constructed that allowed the manipulation of visual information and eliminated haptic information about the impact. The movement task itself was again strictly confined to one dimension and was identical to the original study by Schaal et al. (1996).

Method

Participants

One woman and 2 men (mean age = 33.4 years) volunteered for this experiment. They were graduate and postgraduate students in the lab of the Department for Brain and Cognitive Science at the Massachusetts Institute of Technology. Two were right-handed, 1 was left-handed; the movements were always performed with the dominant hand.

Apparatus and Data Collection

The apparatus with which the movements were performed is shown in Figure 10. The racket was mounted to a pantograph linkage 1.0 m long, and its two hinges were connected to a stanchion 1.0 m high. At the distal end of the linkage a racket surface was mounted. The proximal end of the linkage had an attached handle that the participants held in a fully pronated grip and performed downward movements to produce upward movements of the racket. The racket was a Koosh paddle, a commercially available beach toy. It consisted of a circular frame of .30 m diameter that was covered by an elastic fabric. The coefficient of restitution α was experimentally determined to be .71. The pantograph linkage was a lever arm with a parallelogram-like arrangement such that the racket's surface stayed horizontal during its movement. Participants were positioned behind the handle so that the linkage was horizontally aligned while their forearm and their elbow joint were at an approximately right angle. Although the distal

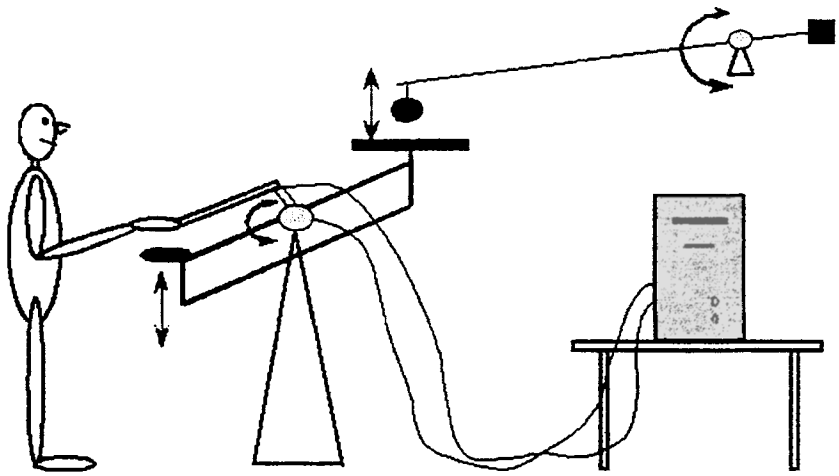

Figure 10. Apparatus used in Experiment 3. The ball was attached to a boom. The apparatus consisted of two handles: One handle was directly attached to the racket surface and was used for the FI (full information) and NO-VI (no visual information) conditions. In the NO-HI (no haptic information) condition, a second identical handle was moved in parallel to the handle proper, and its displacements were recorded by a computer and converted into desired trajectories to be implemented and performed by the proper handle and racket. No information about the impact force of the ball was transferred to the hand.

end of the pantograph's motion was strictly curvilinear, the effective movements of the racket's surface could be considered vertical, because the amplitudes generally did not leave the linear range (±30°).

A table tennis ball with a diameter of 0.03 m was fixed to a light-weight (0.2 kg) aluminum boom 1.0 m long which, in turn, was attached to another stanchion by a hinge joint at a height of 1.2 m. At the boom's opposite short end, a weight could be added, which modified the flight properties of the ball. Boom and racket arm were aligned and arranged so that, in the horizontal position, the ball rested on the center of the racket's surface. A potentiometer, attached to the boom's hinge, measured the angular displacement of the boom that was used to determine the ball's vertical displacement. Similarly, the collection of the position data of the pantograph's movement was done by a high-resolution position encoder that was attached in one of the hinge joints of the stanchion. So far, this is the same apparatus as the one used for the study reported in Schaal et al. (1996).

To create a condition where no haptic information about the impact was available, the above setup was converted into a telerobotic device. For this purpose, a 50 Nm torque motor (NSK Direct Drive, Japan) was added to actuate the original pantograph at its hinge, and an additional 1.0-m-long lever arm was mounted on another stanchion with a hinge joint, positioned in parallel to the pantograph arm. An identical handle was attached to this arm. In the experimental task, participants performed identical up and down movements with this second handle. The angular displacements were measured by a potentiometer, and they were numerically differentiated to obtain velocities. After digital filtering, position and velocity data served as desired trajectories for the torque motor that actually moved the racket on the pantograph as in the original task. The telerobotic connection was operated at 1000 Hz sampling frequency out of a Motorola MVME167 computer running the real-time operating system vxWorks (WindRiver Systems, Alamedo, CA). Because of the high sampling frequency, the time delay between the participants' movements and the racket movements was maximally 5 ms, and the gains of the proportional-derivative controller of the motor could be chosen very high. Consequently, the participants' movements were faithfully reproduced by the robotic device. Given the light weight of the ball–boom setup, impact of racket and ball resulted in minimal deviations of the tracking performance of the robot (i.e., maximal tracking errors were less than 5 mm). Because both the manipulandum's handle and the robot handle were positioned next to each other, the participant perceived the ball's movements as if he or she controlled the handle movement directly. However, the participant had no haptic information about the impact between racket and ball.

The computer collected position data from racket and ball at a sampling frequency of 1000 Hz. Velocity data of ball and racket were derived on-line by numerical differentiation of the position data and subsequent filtering, using a third-order, low-pass Butterworth filter with a cutoff frequency of 30 Hz. Because of memory limitations, only every 10th data point was stored, which corresponded to a downsampling of the data to 100 Hz. Filtering the data on-line at 1000 Hz resulted in a higher bandwidth than off-line filtering of the downsampled data. Delays introduced by the purely forward filters were negligible because of the high sampling frequency. Off-line data processing consisted of high-pass second-order Butterworth filtering of the position data in order to eliminate slow drifting of the average racket position (cutoff frequency .5 Hz, zero-delay filter) and numerical differentiation of the filtered velocity data to derive accelerations for ball and racket.

The dependent measures were determined in the same way as described in Experiments 1 and 2. The central tendency and dispersion for all discrete measures characterizing the periodic trajectory and the impact (i.e., amplitudes, periods, and acceleration at the point of impact) were determined using median and interquartile range of 20 and 34 cycles across each trial. This was done because some trials did not show a normal distribution. Subsequently, the arithmetic means were calculated for two trials per condition of each participant and entered into the analyses of variance.

Experimental Procedure and Design

Prior to the experiment participants were instructed about the task. Participants were given about 5 min to practice using both handles, which was sufficient to make them feel comfortable with the apparatus. During this practice they were asked to explore different amplitudes and frequencies in order to find three distinguishable heights where they could juggle the ball comfortably. The recommendations about the ball amplitudes were identical to Experiment 1. At the beginning of the data collection the participants stood right behind the pantograph, grasping the handle from the top in a pronated grip. Before each trial the participant was informed about the particular amplitude or perceptual condition. Data collection started when the rhythmic movement was stable. If the participant did not maintain a steady rhythm, the trial was repeated. The three perceptual conditions were labeled as *NO-HI* when there was no information about the impact available, *NO-VI* when the participants closed their eyes, and *FI* for full information in the control condition. Each trial lasted 30 s.

A two-factor 3 × 3 design was chosen with three different juggling amplitudes (high, medium, and low) and three perceptual conditions (NO-VI, NO-HI, and FI). Two trials were performed for each of the three amplitude conditions and the three perceptual conditions. Conditions were presented in randomized order. The whole experiment lasted approximately 30 min.

Results and Discussion

Kinematic Description of the Movements of Racket and Ball

Figure 11 gives a first qualitative impression of the coordination of racket and ball in three exemplary trials performed under the three perceptual conditions from top to bottom: full information (FI), no visual information (NO-VI), and no haptic information (NO-HI). Whereas the time series only show a window of 3 s, the accompanying phase portraits on the right display the trajectory across the complete trials. The time series shows the racket's quasi-sinusoidal movements and also illustrates again that the majority of impacts occurred in the decelerating phase. This is similarly represented in the phase portraits where the dots represent the phase of the ball–racket impact. The dots in the upper right quadrant show that impacts were performed with negative $\ddot{x}_R$. Impact at maximum velocity (i.e., zero $\ddot{x}_R$) and impacts with positive $\ddot{x}_R$ are at the top and in the left upper quadrant, respectively. Inspection shows that NO-VI had considerably more dispersed impacts, whereas in the NO-HI condition there was little variation but a noticeable shift in the impacts toward maximum velocity.

The standard kinematic descriptors for ball and racket trajectories were analyzed and are summarized in Table 2. A 3 × 3 repeated measures ANOVA confirmed that participants had no problems to bounce the ball at three distinguishable amplitudes, $F(2, 4) = 25.28$, $p < .01$. The dispersion estimates, the interquartile range of the peak amplitudes IQR(A_B), showed no differences across all six conditions, indicating that participants could produce comparable ball trajectories under all different kinds of perceptual information. On average the IQR(A_B) was 5.5 cm, which corresponded to 10% of the ball amplitude. As listed in Table 2 the NO-HI condition with high ball amplitudes provided considerably more difficulty than all other conditions. When comparing the proportional variability from the table, one can infer that the low amplitude condition was associated with a higher percentage of

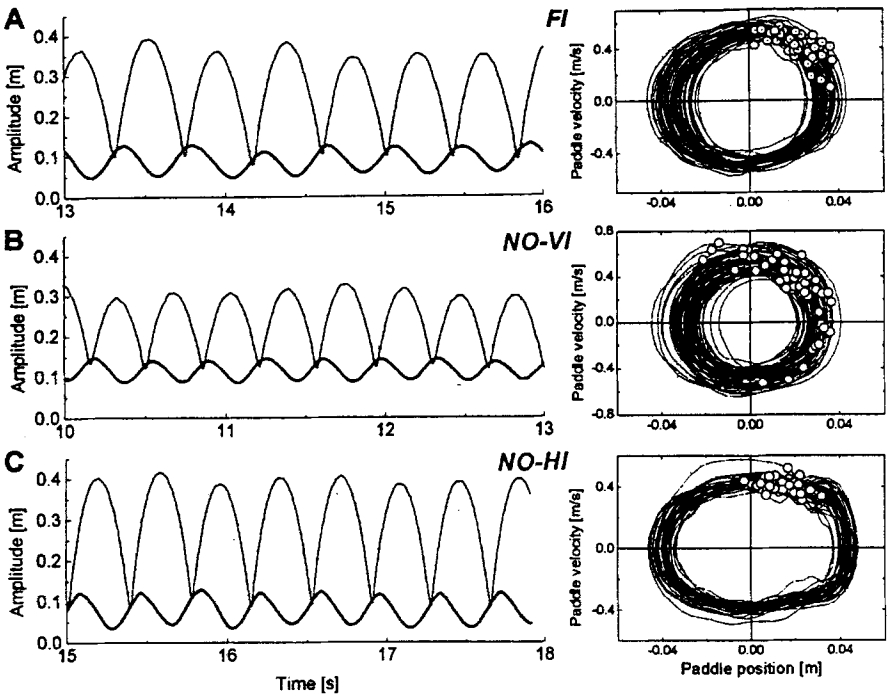

Figure 11. Three time series and their respective phase portraits of exemplary trials performed in the three perceptual conditions of Experiment 3. The dots in the phase portraits denote the impacts. FI = full information condition; NO-VI = no visual information condition; NO-HI = no haptic information condition.

variability in relation to the mean amplitude. A noteworthy finding is that the variability of ball and racket trajectories was not different in the conditions that partially excluded perceptual information.

Racket Acceleration at Impact

We next turned our attention to the acceleration at impact. Median and interquartile ranges served as statistic measures for each trial, and the averages of the two trials per condition were entered into the 3 × 3 repeated measures ANOVAs. The results showed all three effects as significant. A weak interaction identified that whereas $\ddot{x}_R$ successively decreased with decreasing ball amplitude, the medium and high ball amplitudes conditions switched order in the NO-HI condition, $F(4, 8) = 4.06$, $p = .04$ (see Table 2). Because both $\ddot{x}_R$ means were positive, identifying them as unstable trials, this effect was not further interpreted in the present context. The main effect for amplitude revealed that $\ddot{x}_R$ became progressively more negative with lower ball amplitudes, $F(2, 4) = 9.79$, $p < .05$; high, $-.81$ m/s^2; medium, -1.63 m/s^2; low, -3.82 m/s^2. The second main effect for perceptual information showed that in the FI condition $\ddot{x}_R$ was lowest and NO-HI was closest to zero, $F(2, 4) = 8.54$, $p < .05$ (see Table 2). The overall mean values for the three participants in the three perceptual conditions were NO-HI: -0.40 m/s^2; NO-VI: -2.72 m/s^2; FI: -3.15 m/s^2. Post hoc analyses detected a difference between NO-HI and the other two conditions, but no difference between

Table 2
Median (and Interquartile Range) of All Three Participants for Racket Amplitude (A_R; in Meters), Racket Period (T_R; in Seconds), Ball Amplitude (A_B; in Meters), Ball Period (T_B; in Seconds), and Racket Acceleration at Impact ($\ddot{x}_R$; in Meters per Seconds Squared) in Experiment 3

	NO-HI			NO-VI			FI		
Measure	High	Medium	Low	High	Medium	Low	High	Medium	Low
A_R	0.164 (0.016)	0.117 (0.010)	0.065 (0.008)	0.182 (0.027)	0.117 (0.012)	0.071 (0.010)	0.172 (0.014)	0.106 (0.011)	0.065 (0.008)
T_R	0.677 (0.048)	0.556 (0.032)	0.413 (0.021)	0.682 (0.073)	0.576 (0.026)	0.432 (0.022)	0.721 (0.040)	0.552 (0.023)	0.427 (0.020)
A_B	0.627 (0.060)	0.454 (0.037)	0.257 (0.030)	0.646 (0.167)	0.484 (0.041)	0.286 (0.040)	0.694 (0.044)	0.445 (0.038)	0.273 (0.035)
T_B	0.676 (0.043)	0.556 (0.023)	0.416 (0.024)	0.687 (0.107)	0.577 (0.026)	0.433 (0.024)	0.722 (0.034)	0.551 (0.021)	0.427 (0.002)
$\ddot{x}_R$	0.58 (3.28)	1.30 (3.66)	−3.08 (2.65)	−1.27 (6.41)	−2.86 (2.57)	−4.02 (3.09)	−1.74 (2.50)	−3.37 (1.87)	−4.39 (2.61)

Note. NO-HI = no haptic information condition; NO-VI = no visual information condition; FI = full information (control condition).

FI and NO-VI. The mode of all values was at -2.50 m/s^2 (Figure 12).

Turning to the variability estimates IQR($\ddot{x}_R$), the ANOVA identified again all effects as significant. An interaction highlighted that high amplitude bouncing without visual information was more variable than every other condition, $F(2, 4) = 9.16$, $p < .01$. A main effect showed that the variability in the FI condition was significantly lower than in the other two perceptual conditions, $F(2, 4) = 7.61$, $p < .05$. Post hoc tests did not identify differences between NO-HI and NO-VI, but FI was different from the other two. The second main effect revealed that the level of variability increased with increasing amplitude, $F(2, 4) = 7.35$, $p < .05$. Figure 12 summarizes these results graphically by showing all individual trial means and the three overall means for the perceptual conditions. The solid curved line is the superimposed prediction as calculated from the Lyapunov stability analysis although it is only shown for the range of observed values (compare Figure 2). To emphasize that these results were very consistent despite the few participants, we also scrutinized the data for each participant performing under the three perceptual conditions. These arithmetic means of the two trials per condition calculated for the medians of $\ddot{x}_R$ and IQR($\ddot{x}_R$) are listed for each participant in Table 3. In general, the same consistent pattern was observed in all three participants.

In summary, these results were informative with respect to the two major objectives of the study. First, the results confirmed again that in most cases, the predictions from the model were satisfied and participants attuned to the stability properties of the task. Second, examination of the contribution of different perceptual systems to successful task performance showed that the three perceptual conditions led to clearly different results. The results in the control condition FI replicated the findings of the previously published study in which the same apparatus was used in showing a clear consistency with the model's predictions (see Schaal et al., 1996). It also corroborated results from Experiments 1 and 2. In comparison, when continuous visual information was withheld (NO-VI), as in Experiment 1, participants performed with $\ddot{x}_R$ values that were indistinguishable from their performance under no perceptual constraints. Yet, variability in the essential variable was higher in the blindfolded execution, replicating the findings of Experiment 1. In contrast, when continuous visual (i.e., kinematic)

Table 3
Median (and Interquartile Range) of Racket Acceleration at Impact (in Meters per Seconds Squared) for Each Participant in the Three Perceptual Conditions of Experiment 3

Participant	NO-HI	NO-VI	FI
1	0.25 (4.14)	−3.39 (5.02)	−4.08 (2.97)
2	−2.35 (3.05)	−3.97 (4.63)	−3.48 (2.19)
3	0.89 (2.03)	−0.79 (2.40)	−1.90 (1.81)

Note. NO-HI = no haptic information condition; NO-VI = no visual information condition; FI = full information (control condition).

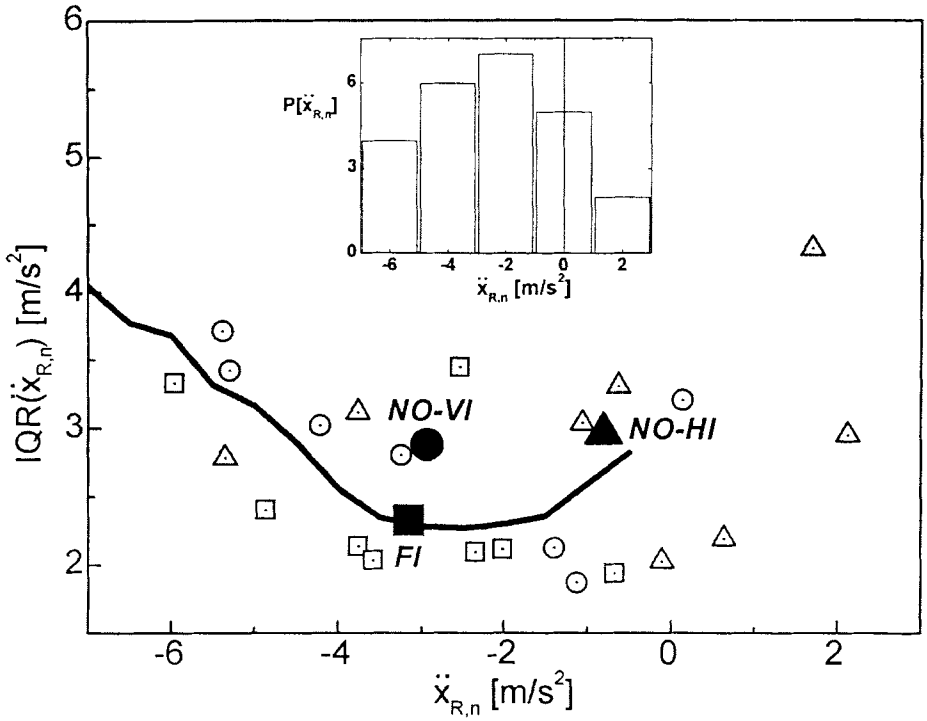

Figure 12. Median and interquartile range (IQR) values of $\ddot{x}_R$ obtained for each trial of all three participants. The enlarged filled symbols represent the means across the three perceptual conditions. The line represents the predicted values from the Lyapunov analysis performed for $\alpha = .71$. The inserted histogram illustrates that the most frequent performance was with $\ddot{x}_R$ values between -6 and -2 m/s^2. NO-VI = no visual information condition; NO-HI = no haptic information condition; FI = full information condition.

information was available, but no haptic (i.e., no kinetic) information about the impact was available (NO-HI), participants performed with $\dot{x}_R$ values that provided less or no stability according to the model. This significant difference is even more interesting when one considers that in the NO-VI condition participants had only intermittent information about the ball location during the very short impacts, compared with uninterrupted visual information in the NO-HI condition.

With respect to our initial hypotheses, these results provide the following answer: Visual information is not crucial for detecting the optimal magnitude of the critical parameter $\dot{x}_R$, but without visual information more variance in performance was observed than in the control condition with full perceptual information. This suggests that during normal performance additional adjustments were made to ensure relative constancy in performance. In addition to visual information, haptic information is the most likely candidate for a central role in the fine-tuning of ongoing performance. Results of the NO-HI condition revealed that searching and maintaining optimal $\dot{x}_R$ values depended more critically on haptic information. In spite of the nonoptimal range of $\dot{x}_R$ values found in the NO-HI trials, variability in $\dot{x}_R$ was not different, a result counter to the model's predictions. For instance, some NO-HI trials with positive $\dot{x}_R$ have even lower variability than NO-VI trials, and this cannot be explained on the basis of the model. What this result clearly expresses is that other strategies such as feedback-based corrections must be used which possibly use visual anticipatory or feedback information to maintain the ball's peak amplitude constant. This observation is in fact very important as it highlights that the dynamically stable strategy is not the only one available. Yet, given our theoretical arguments and empirical support we contend that it is the more parsimonious strategy. With the goal to further reveal signs of such alternative strategies, we conducted a series of analyses on the time series.

Harmonicity

Inspecting the deviations in the racket trajectory from harmonic motion during one cycle of the racket motion, the averaged profiles of λ looked remarkably similar to the ones of Experiment 1 (Figure 7). For all conditions, the phase leading up to the impact at $3\pi/2$ showed positive λ, whereas in the first half of θ_R λ was negative. This clearly speaks to a modulation of the trajectory with respect to the ball. However, all conditions showed the same topology. Variations around the mean profile were uniform throughout the whole cycle. When we performed a 3 × 3 ANOVA on λ_{MSE}, a weak interaction between amplitude and perceptual information marked that for high amplitudes in the haptic condition, λ_{MSE} was significantly higher than in all other conditions, $F(4, 8) = 4.37$, $p < .05$. The measures evidently signaled that for high amplitudes the variability and deviation from harmonicity is larger than for lower amplitudes. There was a main effect of amplitude, indicating that the high amplitude deviated more strongly from a sinusoidal wave than the medium and the low amplitude, $F(2, 4) = 53.96$, $p < .001$.

Relative Phase

As in Experiment 1, the average continuous relative phase between racket and ball was calculated, and the mean profile of each trial was contrasted against the simulated relative phase. As already shown in Figure 8, the profile of relative phase had a distinct shape across one cycle which showed deviations prior to the impact from the simulated profile but did not change in the different conditions. The band of standard deviations showed an increase before and around the impact phase, indicating that adjustments were made directly prior to the impact. However, this signature was indifferent to the experimental manipulations. This picture was reflected in the lack of effects in the cumulative measure ϕ_{MSE} and repeated the lack of effects between perceptual conditions in Experiment 1.

Absolute Position of Impact

Given the unexpected lack of differences between the perceptual conditions in the two preceding analyses of the continuous time series as well as the absence of striking deviations of the trials, classified as unstable in our analyses, we performed a series of other comparisons, one of which did identify differences. Having determined the absolute position of the impact above ground and calculated the median and interquartile range for each trial, we performed a 3 × 3 ANOVA. It identified significant differences between perceptual conditions, $F(2, 4) = 13.52$, $p < .05$, and amplitudes, $F(2, 4) = 15.95$, $p < .01$. Although we expected the decreases in the variability with smaller ball amplitude, the result that the NO-VI condition was less variable than the NO-HI condition was informative about the strategy participants used. In the NO-HI and the FI conditions participants evidently kept the impact position more constant in external space following the instructions to produce an invariant pattern. Without visual information (the NO-VI condition), the impact position varied more in its vertical location. Yet, the acceleration was generally in the range expected to provide more stability. Thus, one can conclude that when participants had no information about the impact force, they emphasized invariance in the kinematic pattern at the expense of the dynamically more optimal impact.

General Discussion

The experimental task of bouncing a ball with a racket is exemplary of the complex demands that coordinated action presents for the individual's perceptual–motor system. In order to bounce the ball rhythmically, the actor has to perform either single-joint or multijoint movements of the arm to precisely time the racket's motions to intercept the ball with the appropriate impact force to achieve invariant ball amplitudes. Information about the ball trajectory and the impact force has to be detected to coordinate the actions appropriately. Our approach aimed to understand movement coordination as one that arises out of the interplay between the actor's movements and the environment in which the actions are situated. This emphasis on the integrated nature of perception and action as the entry point for investigation is a central tenet in ecological psychology, but it has also increasingly come to the forefront in more cognitive approaches (Fowler & Turvey, 1978; Goodale, 1998; Harman, Humphrey, & Goodale, 1999). A particular advantage motivating the choice of this task is that a model could be developed that minimally captures the task-relevant components: the actor's movements represented in terms of a periodically moving surface, the environmental support

in terms of the racket and ball impact, and the ensuing ballistic flight trajectory of the ball.

In the mathematical literature it was shown that a very similar nonlinear impact map displays the typical attractor solutions with a period-doubling route to chaos found in nonlinear maps, similar to the better known logistic map (for an introduction, see Peitgen, Jürgens, & Saupe, 1992; Tufillaro et al., 1992). Our primary hypothesis was that attractor solutions of this system were relevant for human perceptual–motor coordination. We further assumed that dynamic stability of an attractor solution is a meaningful criterion for successful performance, because this solution can potentially alleviate the need for processing-expensive feedback-based control. We therefore conducted two types of stability analysis on the model that provided qualitative and quantitative predictions. Local linear stability analysis identified that the acceleration of the racket at impact was the critical variable that uniquely determined whether the task was performed in a dynamically stable fashion. Nonlocal stability analysis yielded differentiated predictions about the degree of stability associated with different values of acceleration. Borrowing the language of Gel'fand and Tsetlin (1962, 1971), this task, as such, provided an example of a well-organized action problem where an essential variable could be isolated from nonessential ones. Essential variables are collective variables that determine the topology of the solution and that are formulated at a level of description relevant for the actor. The candidate for an essential variable was the acceleration at impact, which then served as the primary criterion to evaluate participants' performance.

Three task variations were designed that corresponded to the simple model system such that the criteria for stable solutions directly served as hypotheses for evaluating the human performance. In a previous article (Schaal et al., 1996) we already presented the ball–table model and tested its validity in a highly constrained task that directly imitated the horizontal surface and the restriction to one-dimensional movements of ball and surface. The results presented a first support for the hypothesis that dynamic stability was an important criterion that guided actors in executing this task. The experiments reported in this article further verified in three task variations that participants chose movement solutions in quantitative and qualitative accordance to the theoretical predictions, even when the task was less constrained. Three very different experimental set-ups involved either full-arm movements (Experiments 1 and 2) or single-joint movements (Experiment 3), with performance constrained to either one dimension (Experiments 1 and 3) or 3-D (Experiment 2). In all cases participants preferred solutions with negative racket acceleration at impact around -3 m/s^2, which predicted highest stability, although other solutions were occasionally chosen. The observed variability in different task measures followed the differential predictions of the Lyapunov stability analysis.

The objective of the incremental relaxing of constraints in the first two experiments was to demonstrate the generality and robustness of these predictions and to probe whether more natural juggling tasks could be addressed with this approach. All results encouraged more research that transfer this approach to other ball manipulative skills such as bouncing a ball on the floor or even catching and throwing actions that involve complex finger and hand coordination. Romack (1995), for instance, showed that in basketball dribbling it is the phasing of the contact between ball and hand trajectory that distinguishes the learners' progress and the influence of different demonstrations. We also believe that the present results are a promising bridge between our simple skill and juggling as investigated by Beek and colleagues (Beek, 1989a, 1989b; Beek & Turvey, 1992; Beek & van Santvoord, 1992). Sternad (1999) reviewed the theoretical and empirical methodologies adopted in both lines of research, showing their parallels and differences. Common in both lines of research is that a theoretical analysis of the task as a dynamical system defined a measurable quantity that successfully served as a benchmark to characterize stable solutions and address questions of movement control, perception, and learning. Where these two lines of research meet remains an open question.

Having established that acceleration at impact is indeed a viable candidate for an essential variable in the actor's coordination, we next searched for the kind of perceptual information that supported the participants' attuning to optimal values of this variable. Experiment 1 contrasted the one-dimensional task performed with and without visual information. It was hypothesized that if the bouncing actions were performed in a dynamically stable regime, then the lack of visual information should not affect task performance, given that self-inflicted deviations remained small. Indeed, the results showed that even when blindfolded, participants continued to choose ball contacts with negative accelerations. We concluded that haptic or maybe even auditory information must have been sufficient to attune to the appropriate acceleration value. On the other hand, increased variability reflected some change in the level of control. Evidently, when full information is available visual information aids in stabilizing task performance. Analysis of the continuous racket trajectory and the relative phase between ball and racket revealed that approximately one quarter cycle prior to contact, there is a marked modulation in relative phase accompanied by increased variability across repeated cycles. We interpreted this finding as indicative of anticipatory adjustments, preparing for the right impact. However, no differences between perceptual conditions could be identified.

Insights that are more conclusive were obtained in Experiment 3, which also permitted the exclusion of haptic information. In this condition, participants had unrestricted information about the ball and racket trajectories as well as about their arm movements. The only missing piece was direct information about the force of the impact. Contrary to our expectation, we found that under this manipulation participants tended not to use or find the dynamically stable strategy, and many trials had to be considered as unstable according to model criteria. This result is noteworthy because a series of studies has accumulated evidence that information about kinetics, specifically in collision events, can be obtained from kinematic (i.e., visual) information (Bingham, 1995; Michaels & de Vries, 1998; Runeson & Frykholm, 1983; Runeson & Vedeler, 1993; Todd & Warren, 1982). In contrast, in our study the intermittent and extremely short moments of impact provided better guidance than visual information to bounce the ball with negative acceleration at impact. That haptic perception reveals more than location and magnitude of contact and pressure on the skin has been shown in a long series of studies on dynamic touch (for an overview, see Turvey, 1996). The haptic system is a complex perceptual system that uses the stress and strain patterns exerted onto muscle tissue including muscular effort in order to perceive object properties that are contacted. Closely related to the present

task is a study by Carello et al. (1999) in which participants detected the location of the sweet spot of a tennis racket. In the experiment, participants reliably reported the distance of the racket's center of percussion (sweet spot) from the hand by merely wielding the racket. This and similar studies highlight the ability of the haptic system of perceiving geometric (distance) and dynamic (center of percussion) properties of hand-held objects. Similar to our experiment this study demonstrates the power of the haptic system which, however, because of its complex nature is not yet as well understood as the visual system, and its contribution is often underestimated.

One final result in Experiment 3 revealed one further point: The position of impact between racket and ball in external space was an uncontrolled part in the task. When visual information was available, participants kept the position relatively stable in absolute coordinates compared to the trials that relied primarily on haptic information. This finding is consistent with the fact that kinesthetic information does not provide position information that is needed to anchor the impact in external space. However, this behavior nevertheless is associated with impacts that are classified as dynamically stable. This finding indicated that in the NO-HI conditions participants tended to freeze the ball-racket system in external space in the attempt to satisfy invariance demands of the instruction, but they sacrificed a dynamically stable impact. In contrast, when only haptic information was available, this invariant impact position was irrelevant and more variable whereas the control of the ball impact remained in the stable range.

To further probe into more subtle differences in the continuous trajectories, we analyzed the limit cycle characteristics of the racket trajectory and relative phasing between ball and racket. The so-called harmonicity measure, which quantified deviations from a harmonic wave, looked remarkably similar in their profiles across all conditions. The only difference was that deviations scaled up for larger amplitude trajectories but did not change in their topological profile. Similarly, relative phase showed remarkable invariance across amplitudes and perceptual variations. This observation is in accordance with the results of Schaal et al. (1996), who proposed a criterion for topological invariance (see also Sternad, 1998). The scaling of movements in size did not change the topology of the endpoint trajectories, even when they were associated with systematic changes in the impact (Bernstein, 1967). It is worth highlighting that, whereas these continuous measures did not identify differences between the different perceptual conditions, the racket acceleration was the most sensitive measure, thus indirectly confirming the validity of this measure.

Negative acceleration at impact is not a trivial result. From an efficiency point of view the ball should be hit at peak velocity (i.e., zero acceleration). The trend toward more negative acceleration values across repetitions in Experiment 1 speaks clearly against this expectation. Conversely, it demonstrates that a strategy in which the ball is hit in its decelerating portion is more preferable and found over practice. This effect is further explored in Sternad and Katsumata (2000) and ongoing research. In fact, when comparing this study to work in robotics, Koditschek and colleagues constructed a one-dimensional juggling robot, consisting of a flat board impacting a puck on a steep inclined plane, which was driven by the so-called *mirror algorithm* (Bühler, Koditschek, & Kindlmann, 1994). This algorithm controlled the actuator's velocity such that it mirrored the ball's velocity (with opposite sign), a strategy that entails positive acceleration for the actuator at impact. The task is equally close to our impact map so that it can be concluded that these are unstable juggling strategies, and, consequently, noise and perturbations required high-performance stabilizing feedback loops. For an artificial system it would undoubtedly be a less computationally expensive strategy if a stable solution had been programmed in the first place.

Our entry into analyzing the skill of bouncing a ball started with modeling the task with a kinematic nonlinear impact map. Although we used the analysis tools of nonlinear dynamics, our strategy differs from what is often referred to as the *dynamic pattern approach* (Kelso, 1995; Turvey, 1990). Interestingly for the present context, this modeling framework was applied to account for a very similar ball-batting task and can serve to illustrate a different modeling strategy (Sim, Shaw, & Turvey, 1997). The central first step in the dynamic pattern approach is the identification of an order parameter, which captures the intrinsic dynamics of the system. Relative phase between the oscillating limbs has been verified to play the role of such an order parameter for rhythmic interlimb coordination. The second step is the formulation of a potential equation for this order parameter that captures the stable states described by the invariant value(s) of this collective variable. To include task demands into the modeling, instruction or intentions were modeled as an additive term in this potential function, setting intrinsic and extrinsic dynamics at the same formal level (Schöner & Kelso, 1988a, 1988b, 1988c). Batting a ball was modeled in this spirit, and relative phase between the ball and bat's periodic movements served as the order parameter. Striking the ball at the preferred frequency and amplitude was captured by a potential equation representing the intrinsic dynamics, and additional task requirements, like hitting the ball against a wall, were added as additional terms representing the extrinsic dynamics. Stability analyses of the model successfully predicted stable phase relationships between ball and bat and the associated degree of stability as a function different parameters.

Yet a different level of dynamic modeling was pursued in the study of three-ball cascade juggling by Beek and colleagues (Beek, 1989a, 1989b; Beek & Turvey, 1992). Instead of attempting to analyze this highly complex coordination of the individual hands and fingers, the authors focussed on a task analysis as their entry into understanding the complex skill. In a series of studies, they identified constraints in the relations between component times of hand and ball trajectories where fundamental relations between component times provided boundaries for which movements are realizable. Formal and empirical analyses gave support to the hypothesis that human jugglers obey principles of dynamics showing that component times of the hand and ball cycles showed properties of phase locking. Additional arguments derived from the theory of phase locking specified a set of particular values as preferable for stable performance. As in the dynamic pattern perspective, no explicit account for the generation of movement in terms of state variables was attempted (for a detailed comparison, see Sternad, 1999). Needless to mention, all three strategies have their merits as well as shortcomings. At this still early stage in the development of dynamical systems tools for analysis of movement coordination, it remains a useful exercise to recognize strategic differences and to be aware of the multiplicity of tools available.

Summary

We analyzed the perceptual–motor task of ball bouncing by adopting a task-based approach with the goal to identify a variable

that is essential in constraining the many degrees of freedom in the task. On the basis of a formal model and analyses from nonlinear dynamics, we hypothesized that dynamic stability is a central aspect that actors tend to use in performance. Stability analyses of the nonlinear model of the ball bouncing system rendered acceleration at impact as candidate for the essential variable. Quantitative and qualitative model predictions about the acceleration at impact were satisfied in three task variations. Manipulation of perceptual information highlighted that performance relied on both visual and haptic information in different ways. Whereas haptic information was the most critical perceptual source in attuning to dynamic stability, visual information provided a constant support to keep performance variability in bounds. From continuous time series analysis we conclude that these perceptual sources present both anticipatory and corrective mechanisms.

References

Amazeen, E. L., Amazeen, P. G., Post, A. A., & Beek, P. J. (1999). Timing in the selection of information during rhythmic catching. *Journal of Motor Behavior, 31,* 279–290.

Arnol'd, V. I. (1983). *Geometrical methods in the theory of ordinary differential equations.* Berlin: Springer Verlag.

Beek, P. J. (1989a). *Juggling dynamics.* Amsterdam, the Netherlands: Free University Press.

Beek, P. J. (1989b). Timing and phase locking in cascade juggling. *Ecological Psychology, 1,* 55–96.

Beek, P. J., & Turvey, M. T. (1992). Temporal patterning in cascade juggling. *Journal of Experimental Psychology: Human Perception and Performance, 18,* 934–947.

Beek, P. J., & van Santvoord, A. A. M. (1992). Learning the cascade juggle: A dynamical systems analysis. *Journal of Motor Behavior, 24,* 85–94.

Bernstein, N. (1967). *Coordination and regulation of movements.* New York: Pergamon Press.

Bingham, G. P. (1995). Dynamics and the problem of visual event recognition. In R. Port & T. van Gelder (Eds.), *Mind as motion: Dynamics, behavior, and cognition* (pp. 403–448). Cambridge, MA: MIT Press.

Bootsma, R. J., & van Wieringen, P. C. W. (1990). Timing an attacking forehand drive in table tennis. *Journal of Experimental Psychology: Human Perception and Performance, 16,* 21–29.

Bühler, M., Koditschek, D. E., & Kindlmann, P. J. (1994). Planning and control of a juggling robot. *International Journal of Robotics Research, 13,* 101–118.

Carello, C., Thuot, S., Anderson, K. L., & Turvey, M. T. (1999). Perceiving the sweet spot. *Perception, 28,* 307–320.

Celaschi, S., & Zimmermann, R. L. (1987). Evolution of a two-parameter chaotic dynamics from universal attractors. *Physics Letters A, 120,* 447–451.

Chen, T.-C. (1984). *Linear systems theory and design.* Orlando, FL: Holt, Rinehart and Winston.

de Oliveira, C. R., & Goncalves, P. S. (1997). Bifurcations and chaos for the quasiperiodic bouncing ball. *Physical Review E, 56,* 4868–4871.

Elliott, B. C. (2000). Hitting and kicking. In V. Zatsiorsky (Ed.), *Biomechanics in sport* (pp. 487–504). Oxford, England: Blackwell Science.

Fowler, C. A., & Turvey, M. T. (1978). Skill acquisition: An event approach with special reference to searching for the optimum of a function of several variables. In G. E. Stelmach (Ed.), *Information processing in motor control and learning* (pp. 1–40). New York: Academic Press.

Gel'fand, I. M., & Tsetlin, M. L. (1962). Some methods of control for complex systems. *Russian Mathematical Surveys, 17,* 95–116.

Gel'fand, I. M., & Tsetlin, M. L. (1971). Mathematical modeling of mechanisms of the central nervous system. In I. M. Gel'fand, V. S. Gurfinkel, S. V. Fomin, & M. T. Tsetlin (Eds.), *Models of the structural-functional organization of certain biological systems* (pp. 1–22). Cambridge, MA: MIT Press.

Gibson, J. J. (1966). *The senses considered as perceptual systems.* Boston, MA: Houghton Mifflin.

Gibson, J. J. (1979). *The ecological approach to visual perception.* Boston, MA: Houghton Mifflin.

Goodale, M. A. (1998). Vision for perception and vision for action in the primate brain. *Novartis Foundation Symposium, 218,* 21–34.

Greene, P. H. (1967). Seeking mathematical models for skilled actions. In D. Bootzin & H. C. Muffley (Eds.), *Biomechanics: Proceedings of the first Rock Island Arsenal Biomechanics Symposium* (pp. 149–180). New York: Plenum Press.

Greene, P. H. (1972). Problems of organization of motor systems. In R. Rosen & F. Snell (Eds.), *Progress in theoretical biology* (Vol. 2, pp. 1.1–6.12). New York: Academic Press.

Guckenheimer, J., & Holmes, P. (1983). *Nonlinear oscillations, dynamical systems, and bifurcations of vector fields.* New York: Springer.

Harman, K. L., Humphrey, G. K., & Goodale, M. A. (1999). Active manual control of object views facilitates visual recognition. *Current Biology, 9,* 1315–1318.

Herring, R. M., & Chapman, A. E. (1982). Effects of changes in segmental values and timing of both torque and torque reversal in simulated throws. *Journal of Biomechanics, 25,* 1173–1184.

Hongler, M.-O., Cartier, P., & Flury, P. (1989). Numerical study of a model of vibro-transporter. *Physics Letters A, 135,* 106–112.

Hubbard, M., Covarrubias, J. R., Hagenau, W., & Jenssen, C. (1989). Ball impact mechanics: Biomechanical implications. In R. J. Gregor, R. F. Zernicke, & W. C. Whiting (Eds.), *Proceedings of the XIIth International Congress of Biomechanics* (Abstract No. 279). Los Angeles: University of California, Los Angeles.

Jackson, E. A. (1989). *Perspectives of nonlinear dynamics* (Vol. 1). New York: Cambridge University Press.

Kelso, J. A. S. (1995). *Dynamic patterns: The self-organization of brain and behavior.* Cambridge, MA: MIT Press.

Kowalik, Z., Franaszek, M., & Pieranski, P. (1988). Self-reanimating chaos on the bouncing-ball system. *Physical Review A, 37,* 4016–4022.

Lichtenberg, A. J., & Lieberman, M. A. (1982). *Regular and stochastic motion.* New York: Springer-Verlag.

Michaels, C. F., & de Vries, M. M. (1998). Higher order and lower order variables in the visual perception of relative pulling force. *Journal of Experimental Psychology: Human Perception and Performance, 24,* 526–546.

Peitgen, H.-O., Jürgens, J. H., & Saupe, D. (1992). *Chaos and fractals: New frontiers of science.* New York: Springer.

Pieranski, P., & Bartolino, R. (1985). Jumping particle model. Modulation modes and resonant response to a periodic perturbation. *Journal de Physique, 46,* 687–690.

Pieranski, P., Kowalik, Z., & Franaszek, M. (1985). Jumping particle model. A study of the phase space of a non-linear dynamical system below its transition to chaos. *Journal de Physique, 46,* 681–686.

Press, W. P., Flannery, B. P., Teukolsky, S. A., & Vetterling, W. T. (1988). *Numerical recipes in C—The art of scientific computing.* Cambridge, MA: Press Syndicate University of Cambridge.

Romack, J. L. (1995). *Observational learning and acquisition of complex motor patterns by children: A perception/action approach.* Unpublished doctoral dissertation, Department of Kinesiology, Indiana University, Bloomington, IN.

Runeson, S., & Frykholm, G. (1983). Kinematic specification of dynamics as an informational basis for person-and-action perception: Expectation, gender recognition, and deceptive intention. *Journal of Experimental Psychology: General, 112,* 585–615.

Runeson, S., & Vedeler, D. (1993). The indispensability of precollision kinematics in the visual perception of relative mass. *Perception & Psychophysics, 53,* 617–632.

Schaal, S., Sternad, D., & Atkeson, C. G. (1996). One-handed juggling: A dynamical approach to a rhythmic movement task. *Journal of Motor Behavior, 28,* 165–183.

Schöner, G., & Kelso, J. A. S. (1988a, March 25). Dynamic pattern generation in behavioral and neural systems. *Science, 239,* 1513–1520.

Schöner, G., & Kelso, J. A. S. (1988b). Dynamic patterns of biological coordination: Theoretical strategy and new results. In J. A. S. Kelso, A. J. Mandell, & M. F. Shlesinger (Eds.), *Dynamic patterns in complex systems* (pp. 77–102). Singapore: World Scientific.

Schöner, G., & Kelso, J. A. S. (1988c). Synergetic theory of environmentally specified and learned patterns of movement coordination. 2. Component oscillator dynamics. *Biological Cybernetics, 58,* 81–89.

Sim, M., Shaw, R. E., & Turvey, M. T. (1997). Intrinsic and required dynamics of a simple bat-ball skill. *Journal of Experimental Psychology: Human Perception and Performance, 23,* 101–115.

Simmons, G. E. (1985). *Calculus with analytical geometry.* New York: McGraw-Hill.

Sternad, D. (1998). A dynamic systems perspective to perception and action. *Research Quarterly, 69,* 319–326.

Sternad, D. (1999). Juggling and bouncing balls: Parallels and differences in dynamic concepts and tools. *International Journal of Sports Psychology, 30,* 462–489.

Sternad, D., Duarte, M., Katsumata, H., & Schaal, S. (2000). Dynamics of a bouncing ball in human performance. *Physical Review E, 63,* 011902.1–011902.8.

Sternad, D., & Katsumata, H. (2000). The role of dynamic stability in the acquisition and performance of a rhythmic skill. In J. Raczek, Z. Waskiewicz, & G. Juras (Eds.), *Current research in motor control* (pp. 55–62). Katowice, Poland: Interaktiv SC.

Sternad, D., Turvey, M. T., & Saltzman, E. L. (1999). Dynamics of 1:2 coordination in rhythmic interlimb movement. I. Generalizing relative phase. *Journal of Motor Behavior, 31,* 207–223.

Strogatz, S. H. (1994). *Nonlinear dynamics and chaos.* Reading, MA: Addison-Wesley.

Todd, J. T., & Warren, W. H. (1982). Visual perception of relative mass in dynamic events. *Perception, 11,* 325–335.

Tufillaro, N. B., Abbott, T., & Reilly, J. (1992). *An experimental approach to nonlinear dynamics and chaos.* Redwood City, CA: Addison–Wesley.

Turvey, M. T. (1990). Coordination. *American Psychologist, 45,* 938–953.

Turvey, M. T. (1996). Dynamic touch. *American Psychologist, 51,* 1134–1152.

van Santvoord, A. A. M., & Beek, P. J. (1994). Phasing and the pickup of optical information in cascade juggling. *Ecological Psychology, 6,* 239–263.

Appendix A

Modeling the Bouncing Ball System as an Impact Map

To formulate a model for a bouncing ball, we express the motions of ball and racket in terms of two state vectors, describing position and velocity of ball and racket, respectively:

$$\mathbf{x}_B = (x_B, \dot{x}_B)^T$$

$$\mathbf{x}_R = (x_R, \dot{x}_R)^T. \tag{A1}$$

The subscripts B and R refer to the ball and racket, respectively. This contrasts to the dimensionless form of the classical dissipative standard map, known as the *modified Fermi-Ulam problem* (Lichtenberg & Lieberman, 1982) but facilitates comparison of the model with actual data. The motion is confined to the vertical dimension, where a positive sign defines the upward direction. The instantaneous impact is defined by

$$\alpha(\dot{x}_R - \dot{x}_B) = -(\dot{x}'_R - \dot{x}'_B), \tag{A2}$$

where the prime denotes the variables immediately after the impact. Alpha is the coefficient of restitution capturing the energy loss during impact. Under the assumption that $\dot{x}_R = \dot{x}'_R$, which implies that the mass of the racket is much larger than the ball, $m_R \gg m_B$, the impact relation can be rewritten:

$$\dot{x}'_B = \dot{x}_R(1 + \alpha) - \alpha\dot{x}_B. \tag{A3}$$

To render the analysis tractable, the continuous dynamical equations of motion are discretized at the point immediately before the ball–racket impact. At this moment both x_R and x_B are identical and collapse into one state, thus reducing the dimensionality of the system by one. This discretization is equivalent to taking the Poincare section at $\Sigma = \{(x_B, x_R) \in R^4 | x_B - x_R = 0\}$. Information about the stability properties of the continuous ball–racket system is completely contained in the recurrent pattern of the discrete points of impact. Using the equations for ballistic flight

$$\ddot{x}_B = -g, \tag{A4}$$

$$\dot{x}_B = -gt + c_1, \text{ and} \tag{A5}$$

$$x_B = -1/2gt^2 + c_1t + c_2, \tag{A6}$$

where g is the gravitational constant, and setting time to zero at every impact after a cycle period T, we can write $\dot{x}_B(t = 0) = \dot{x}'_{B,n}$ and $x_B(t = 0) = x_{B,n}$ and solve for the coefficients $c_1 = \dot{x}'_{B,n}$ and $c_2 = x_{B,n}$. The subscripts n denote the successive impacts. Inserting the coefficients into Equation A6 the position of the ball at impact $n + 1$ (which, by definition, equals the one of the racket) can now be expressed from the assumption of a ballistic flight of the ball:

$$x_{B,n+1} = x_{R,n+1} = -1/2gT^2 + \dot{x}'_{B,n}T + x_{B,n} \tag{A7}$$

and solved for T:

$$T = -1/g(-\dot{x}'_{B,n} - \sqrt{(\dot{x}'_{B,n})^2 + 2g(x_{R,n} - x_{R,n+1})}) \tag{A8}$$

Note that we omitted the second solution of Equation A7 in Equation A8 (i.e., a solution that would have a negative T), because it is irrelevant for our experiments. Following from

$$\dot{x}_B = -gt + \dot{x}'_{B,n} \text{ and}$$

$$\dot{x}_B(T) = -gT + \dot{x}'_{B,n}, \tag{A9}$$

a discrete equation for ball velocity can be derived by inserting Equation A8 into Equation A9:

$$\dot{x}_{B,n+1} = \dot{x}_B(T) = -\sqrt{(\dot{x}'_{B,n})^2 + 2g(x_{R,n} - x_{R,n+1})} \tag{A10}$$

Inserting the impact relation (Equation A3) into the derived expressions yields the final set of system equations:

$$\dot{x}_{B,n+1} = -\sqrt{((1 + \alpha)\dot{x}_{R,n} - \alpha\dot{x}_{B,n})^2 + 2g(x_{R,n} - x_{R,n+1})}$$

$$x_{B,n+1} = x_{R,n+1}$$

$$x_{R,n+1} = x_{R,n}(T) \text{ where } T \text{ results from}$$

$$-1/2gT^2 + ((1 + \alpha)\dot{x}_{R,n} - \alpha\dot{x}_{B,n})T + (x_{R,n} - x_{R,n+1}) = 0. \tag{A11}$$

Appendix B

Stability Analyses of the Bouncing Ball System

Local Linear Stability

Local linear stability analysis gives a first assessment of the stability properties of the fixed points determined for the model system (Equations 1 and A11). We prove stability under the assumption that the racket's trajectory is an arbitrary periodic motion, formalized by a finite Fourier series:

$$x_R(t) = \sum_{r=1}^{K} A_r \sin(r\omega t + \varphi_r),$$

such that at impact, position, velocity, and acceleration of the racket can be written as

$$x_{R,n} = \sum_{r=1}^{K} A_r \sin(r\omega t_n + \varphi_r) = f(\omega t_n),$$

$$\dot{x}_{R,n} = \omega \sum_{r=1}^{K} A_r r \cos(r\omega t_n + \varphi_r) = \omega f'(\omega t_n), \text{ and}$$

$$\ddot{x}_{R,n} = \omega^2 \sum_{r=1}^{K} - A_r r^2 \sin(r\omega t_n + \varphi_r) = \omega^2 f''(\omega t_n),$$

respectively, where A denotes the amplitude, ω denotes the angular velocity, and φ denotes the phase. Using these equations and defining the phase of the racket at the moment of impact as $\theta_n = \omega t_n \pmod{2\pi}$, we reformulate the racket states at impact in compact form as

$$x_{R,n} = f(\theta_n)$$

$$\dot{x}_{R,n} = \omega f'(\theta_n)$$

$$\ddot{x}_{R,n} = \omega^2 f''(\theta_n)$$

where

$$f'(\theta_n) = \frac{\partial}{\partial \theta_n} f(\theta_n) \text{ and } f''(\theta_n) = \frac{\partial^2}{\partial \theta_n^2} f(\theta_n)$$

The discrete equations of the racket-ball system from Equation A11 can thus be replaced in terms of a function of the phase and ball velocity:

$$\dot{x}_{B,n+1} = -\sqrt{((1+\alpha)\omega f'(\theta_n) - \alpha \dot{x}_{B,n})^2 + 2g(f(\theta_n) - f(\theta_{n+1}))}$$

$$\theta_{n+1} = \theta_n + T\omega \qquad \text{(B1)}$$

where T results from

$$-1/2gT^2 + ((1+\alpha)\omega f'(\theta_n) - \alpha \dot{x}_{B,n})T + f(\theta_n) - f(\theta_{n+1}) = 0.$$

The equilibrium points of this discrete dynamical system must fulfill the conditions $\theta_{n+1} = \theta_n$ and $\dot{x}_{B,n+1} = \dot{x}_{B,n}$, resulting in the equilibrium conditions:

(i) $\omega T = 2\pi = \text{constant}$

(ii) $\dot{x}_{B,n} = -\frac{1}{2} gT \; (<0)$

(iii) $\dot{x}_{R,n} = \omega f'(\theta_n) = \frac{1}{2} gT \frac{(1-\alpha)}{(1+\alpha)} \; (>0).$

Defining the state of the dynamical system in Equation B1 as

$$\mathbf{z}_n = \begin{pmatrix} \dot{x}_{B,n} \\ \theta_n \end{pmatrix},$$

linearization about an equilibrium point results in a matrix equation

$$\mathbf{z}_{n+1} = \mathbf{A}\mathbf{z}_n = \begin{pmatrix} \alpha^2 & -(1+\alpha)\alpha\omega f''(\theta_n) \\ -\dfrac{\alpha\omega(1+\alpha)}{g} & 1 + \dfrac{\omega^2(1+\alpha)^2 f''(\theta_n)}{g} \end{pmatrix} \mathbf{z}_R. \qquad \text{(B2)}$$

This linearization is possible despite the transcendental structure of T in Equation B1 by applying the implicit function theorem. (The implicit function theorem explains how to take the derivative dy/dx of a function, which is in implicit form $f(x, y) = 0$. See, e.g., Simmons, 1985.) The 2×2 matrix $\mathbf{A}$ has two eigenvalues λ_1, λ_2. The condition for stable equilibrium points in discrete systems is that the absolute value of both eigenvalues must lie in the interval [0, 1]. It therefore suffices to test the larger absolute eigenvalue $|\lambda_{\max}|$ for this condition and distinguish among the following three stability cases within the range of $\ddot{x}_{R,n}$:

(a) for $0 > \ddot{x}_{R,n} \geq -g\frac{(1-\alpha)^2}{(1+\alpha)^2}$: $\quad 1 > |\lambda_{\max}| \geq \alpha,$

(b) for $-g\frac{(1-\alpha)^2}{(1+\alpha)^2} > \ddot{x}_{R,n} > -g$: $\quad |\lambda_1 = \lambda_2 = \lambda_{\max}| = \alpha,$

(c) for $-g \geq \ddot{x}_{R,n} > -2g\frac{1+\alpha^2}{(1+\alpha)^2}$: $\quad 1 > |\lambda_{\max}| \geq \alpha.$

The equations show that local stability depends only on the racket's acceleration at impact, $\ddot{x}_{R,n}$, the coefficient of restitution, α, and the gravitational constant g. Whereas α and g are constant and are not under control of an effector system, $\ddot{x}_{R,n}$ serves as the main variable for the assessment of different bouncing solutions in the experiment. For the analytical evaluation of local stability, the range of $\ddot{x}_{R,n}$, where $|\lambda_{\max}|$ is at a minimum, is of primary importance. For given values of α (e.g., .42), the range is [−11.44, 0 m/s^2]. This range is rather large, and local stability analysis does not differentiate between conditions. Hence, a nonlocal stability analysis is required to differentiate between these locally stable solutions. However, a prerequisite for this analysis is that different solutions can be compared (i.e., normalized such that quantitative comparisons are possible). Mathematically, this question is addressed by topological orbital equivalence (TOE), which tests whether one dynamical system can be continuously transformed into another one.

Topological Orbital Equivalence

A formal way of establishing TOE is to find an orientation-preserving homeomorphism between two dynamical systems (Arnol'd, 1983; Jackson, 1989). The following scaling relation h

(*Appendix continues*)

$$h: = \begin{cases} \dot{x}'_{B,n} = c\dot{x}_{B,n} \\ \dot{x}'_{R,n} = c\dot{x}_{R,n} \\ x'_{R,n} = c^2 x_{R,n} \\ t'_n = ct_n \ (\Rightarrow \tau' = c\tau), \end{cases} , c > 0 \qquad \text{(B3)}$$

fulfills the requirements of TOE for Equation 1. For any constant, c, the primed variables also fulfill Equation 1, which can be verified by inserting them into these equations. This implies that by choosing $c = 1/t_n$, each periodic bouncing ball system is normalized by h to unit period without changing its dynamical properties. Hence, because of h, any further analysis of ball bouncing can be performed on one system with unit period. For the present analyses, it is important that the scaling relation does not affect the acceleration of the racket. Thus, acceleration at impact can directly serve as a measure of local stability.

Nonlocal Stability

To obtain a differentiation of stability predictions across the range of $\ddot{x}_{R,n}$, the most common method is a global stability analysis of an equilibrium point that finds a Lyapunov function. This Lyapunov function is a function of the state variables and is formulated such that it has a unique global minimum at this equilibrium point. If the time derivative of this function is always negative (i.e., its value monotonically decreases with time) the system converges to the minimum of the Lyapunov function. According to our definition above, the minimum is the equilibrium point; thus, global stability of the system is proven. For a nonlinear system a Lyapunov function candidate can be derived from the linearized system. The candidate function, L_n, for the linearized dynamical system is (e.g., Chen, 1984)

$$L_n = \mathbf{z}_n^T \mathbf{P} \mathbf{z}_n. \qquad \text{(B4)}$$

To obtain negative time derivatives the matrix $\mathbf{P}$ has to satisfy the equation:

$$\mathbf{A}^T\mathbf{P}\mathbf{A} - \mathbf{P} = -\mathbf{I} \qquad \text{(B5)}$$

$\mathbf{A}$ is the system matrix of Equation A1 and $\mathbf{I}$ is the identity matrix, such that the coefficients of $\mathbf{P}$ can be calculated from the constraint formulated in Equation B5. For the discretized system, the value of L_n must continuously decrease when $\mathbf{x}_{B,n}$ is recursively iterated through Equation B2. Thus, a ΔL can be defined between two successive impacts n and $n + 1$ of ball and racket:

$$\Delta L = L_{n+1} - L_n = \mathbf{z}_{n+1}^T \mathbf{P} \mathbf{z}_{n+1} - \mathbf{z}_n^T \mathbf{P} \mathbf{z}_n, \qquad \text{(B6)}$$

where the nonlinear system Equation B1 must be inserted for $\mathbf{x}_{B,n+1}$. For any state $\mathbf{x}_{B,n}$, ΔL may serve as a measure of how quickly the ball converges to the stable equilibrium point. Whereas negative values of ΔL indicate that $\mathbf{x}_{B,n}$ lies in the basin of attraction, a single positive ΔL characterizes $\mathbf{x}_{B,n}$ as unstable. For the following numerical assessment of stability, we are not able to prove true global stability but rather only nonlocal stability (i.e., a measure of stability in the vicinity of the equilibrium point). As we demonstrate, this numerical analysis suffices to determine the point of maximal robustness for the ball bouncing task.

Using numerical optimization analysis (see below), it is possible to assess nonlocal stability properties by simulating the dynamics of the ball bouncing system given by Equation 1. At time $t = 0$, we defined an equilibrium point to be at the impact position, $x_R = 0$, and the bouncing period was set to $\tau = 0.4$ s. The scaling relation h ensures that these values can be chosen arbitrarily without losing generality of the results. The locally relevant section of the racket trajectory around the equilibrium point was modeled as a sixth order polynomial in time. The order 6 was empirically determined to give sufficient accuracy for the given purpose.

$$x_R(t) = c_o + c_1 t + c_2 t^2 + c_3 t^3 + c_4 t^4 + c_5 t^5 + c_6 t^6 \qquad \text{(B7)}$$

For the given impact conditions, $x_R(t = 0) = 0$, c_0 must be zero. The constant c_1 is also determined, because the racket velocity at impact is fully determined by the ballistic flight and the coefficient of restitution. At impact the second derivative of Equation B7, $\ddot{x}_R(t = 0) = 2c_2$. This acceleration was set to 20 different values, taken from the range of local stability. The goal of the optimization was to adjust the constants c_3 to c_6 for each of the 20 $\ddot{x}_R(t = 0)$ to achieve the largest and steepest basin of attraction for the equilibrium point. Values of ΔL were calculated by starting the ball at 2,500 different initial conditions in the vicinity of the equilibrium point. The sum of all 2,500 ΔLs for a given set of parameters, $\Sigma\Delta L$, was defined as an operational measure quantifying stability for each $\ddot{x}_R(t = 0)$. The ball's initial conditions were determined by different deviations from the impact time, $t = 0$, and impact velocities around the equilibrium point of $\ddot{x}_R$. The range of the initial values was chosen to cover an appropriately large neighborhood around the equilibrium point, but, as this calculation aimed to give relative evaluations of $\ddot{x}_R(t)$, the actual range limits could be chosen freely: $t_{init} \in [-0.18\tau, +0.18\tau]$, $\dot{x}_{B,init} \in [-4m/s, -1m/s]$. The initial conditions were obtained by discretizing the intervals into 50 values each. The optimization was performed with Powell's conjugate gradient method (Press, Flannery, Teukolsky, & Vetterling, 1988).

Figure 2 shows the numerical results of $\Sigma\Delta L$ as a function of $\ddot{x}_R(t)$. Note that small $\Sigma\Delta L$ correspond to high global stability. As the trajectory of the racket corresponding to each of the different $\ddot{x}_R(t)$ was optimized to obtain maximal stability, the results express the best possible case for each $\ddot{x}_R(t)$.

Stability is closely related to variability, because weakly stable states are accompanied with larger fluctuations than highly stable states and have longer relaxation times when perturbed. Therefore, the variability of $\ddot{x}_{R,n}$ should increase proportional to the numerical estimate of the global stability index, $\Sigma\Delta L$.

Received September 8, 1999
Revision received November 29, 2000
Accepted December 20, 2000 ■